

Shining a light into the world's deepest caves: phylogenetic systematics of the troglobiotic scorpion genus *Alacran* Francke, 1982 (Typhlochactidae : Alacraninae)

Carlos E. Santibáñez-López^{A,C}, Oscar F. Francke^A and L. Prendini^B

^AColección Nacional de Arácnidos, Instituto de Biología, Circuito exterior s/n, Ciudad Universitaria, Copilco, Coyoacán A.P. 70-233, Distrito Federal, C.P. 04510, México.

^BScorpion Systematics Research Group, Division of Invertebrate Zoology, American Museum of Natural History, Central Park West at 79th Street, New York, NY 10024-5192, USA.

^CCorresponding author. Email: ironc81@hotmail.com

Abstract. The scorpion genus *Alacran* Francke, 1982, endemic to eastern Mexico, was created to accommodate *Alacran tartarus* Francke, 1982. This remarkable troglobiotic species is adapted for life in some of the world's deepest caves, 720–916 m below the surface in the Sistema Huautla of the state of Oaxaca (the deepest records at which a scorpion has been found). A second species, *Alacran chamuco* Francke, 2009, was later described from Te Cimutaá, also in Oaxaca. In the present contribution, we describe a third species, *Alacran triquimera*, sp. nov., recently discovered in a cave system in the state of Puebla, and test the monophyly and internal relationships of *Alacran*, based on a cladistic analysis of 10 terminal taxa (including seven species representing all four genera of Typhlochactidae) and 151 informative morphological characters, building on a previously published matrix. The single most parsimonious tree obtained, supports the monophyly of *Alacran* and the following relationships among its component species: (*A. chamuco* (*A. tartarus* + *A. triquimera*, sp. nov.)). The phylogenetic relationships among the three species of *Alacran* are consistent with the biogeographical history of the caves they inhabit. Based on the geological history of the Sierra Madre del Sur and the likely similar speleogenesis of the Tres Quimeras, Sistema Huautla and Te Cimutaá caves, we propose a vicariance hypothesis to account for the disjunct distribution of the three species of *Alacran*, whereby an initially more widespread, panmictic ancestral population speciated into three geographically isolated taxa following fragmentation of the southern Sierra Madre del Sur.

Additional keywords: Chelicerata, Arachnida, phylogeny, biogeography, troglomorphism, caves.

Received 10 July 2014, accepted 15 September 2014, published online 19 December 2014

Introduction

The scorpion genus *Alacran* Francke, 1982 (Typhlochactidae Mitchell, 1971), endemic to the central area of the Sierra Madre Oriental in eastern Mexico (Fig. 1), was created to accommodate a remarkable troglobiotic species adapted for life in some of the world's deepest caves. *Alacran tartarus* Francke, 1982 has been collected at depths of 720–916 m below the surface in the Sistema Huautla of the state of Oaxaca, the deepest records at which a scorpion has been found (Francke 1982; Vignoli and Prendini 2009).

In a broader study of Typhlochactidae, Vignoli and Prendini (2009) and Prendini *et al.* (2010) revised *Alacran*, tested its phylogenetic position, and created Alacraninae Vignoli and Prendini, 2009 to accommodate it. A second species of the genus, *Alacran chamuco* Francke, 2009, not included in the analysis of Prendini *et al.* (2010), was later described.

In the present contribution, we describe a third species, *Alacran triquimera*, sp. nov. (Fig. 2), recently discovered in a cave system in the state of Puebla, based on five adult males and

five females (four adult, one subadult and one juvenile), and test the monophyly and internal relationships of the three species of *Alacran*, building on the morphological data matrix of Prendini *et al.* (2010) by adding *A. chamuco* and *A. triquimera*, sp. nov.

The three troglobiotic species of *Alacran* display a disjunct geographical distribution in three separate caves or cave-systems (Fig. 1), in distinct sub-provinces of the Sierra Madre del Sur, i.e. the Sierra Negra in Puebla (*A. triquimera*, sp. nov.), the Sierra Mazateca in Oaxaca (*A. tartarus*) and the Sierra de Juarez, also in Oaxaca (*A. chamuco*). We review the biogeographical history of the caves inhabited by the three species of *Alacran*, explore the question of how their disjunct distribution originated, and propose a hypothesis for their speciation consistent with the results of the cladistic analysis.

Materials and methods

Taxonomy

Material examined is deposited in the following collections: American Museum of Natural History, New York (AMNH),

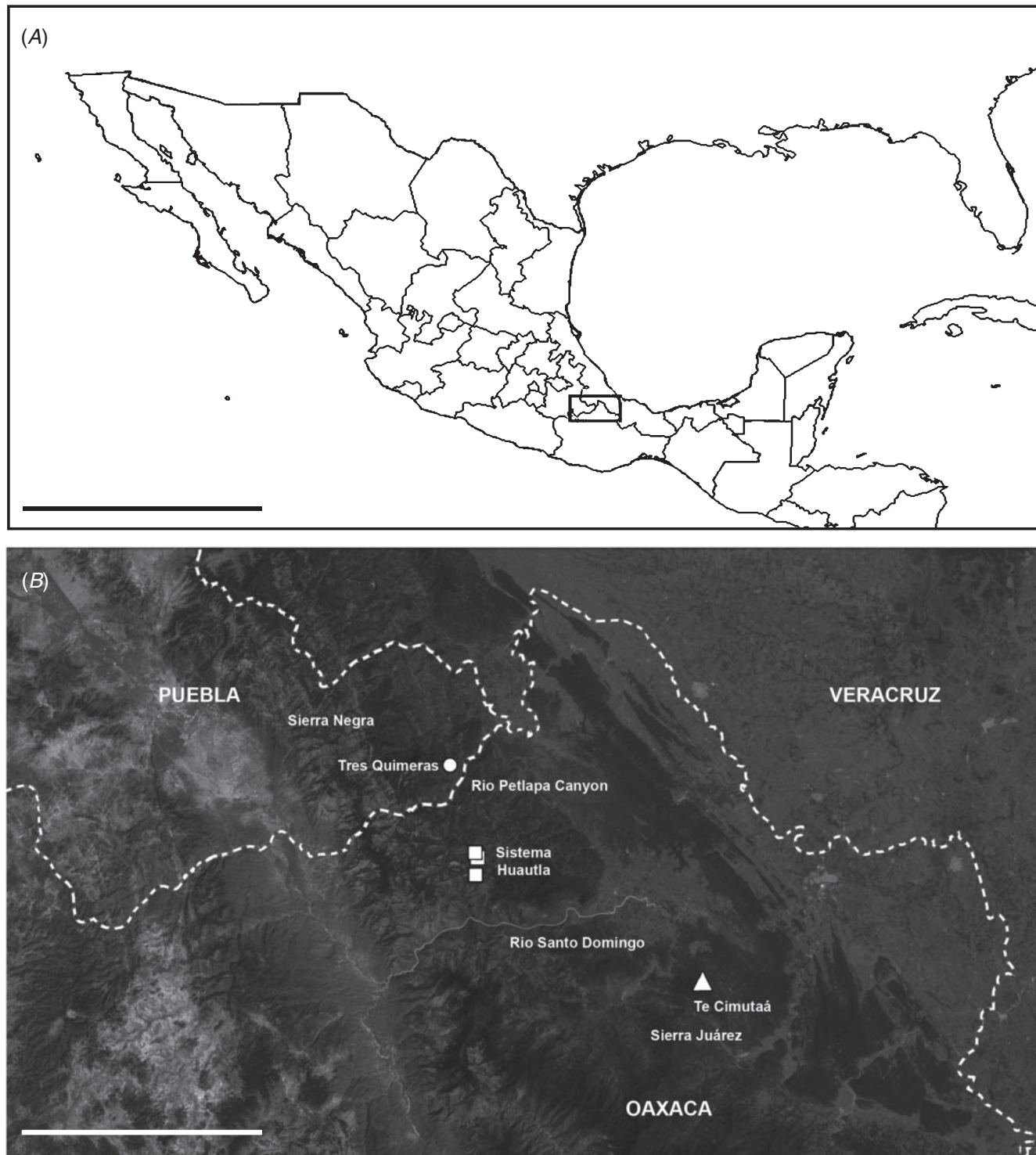


Fig. 1. Map of Mexico (A), plotting known locality records of the three species of *Alacran* Francke, 1982 with major landforms indicated (B): *Alacran chamuco* Francke, 2009 (triangle); *Alacran tartarus* Francke, 1982 (squares); *Alacran triquimera*, sp. nov. (circle). Scale bars = 1000 km.

including the Ambrose Monell Cryocollection for Molecular and Microbial Research (AMCC); California Academy of Sciences, San Francisco (CAS); Colección Nacional de

Arácnidos, Instituto de Biología, Universidad Nacional Autónoma de México, Mexico City (CNAN); Instituto de Investigación de Recursos Biológicos Alexander Von

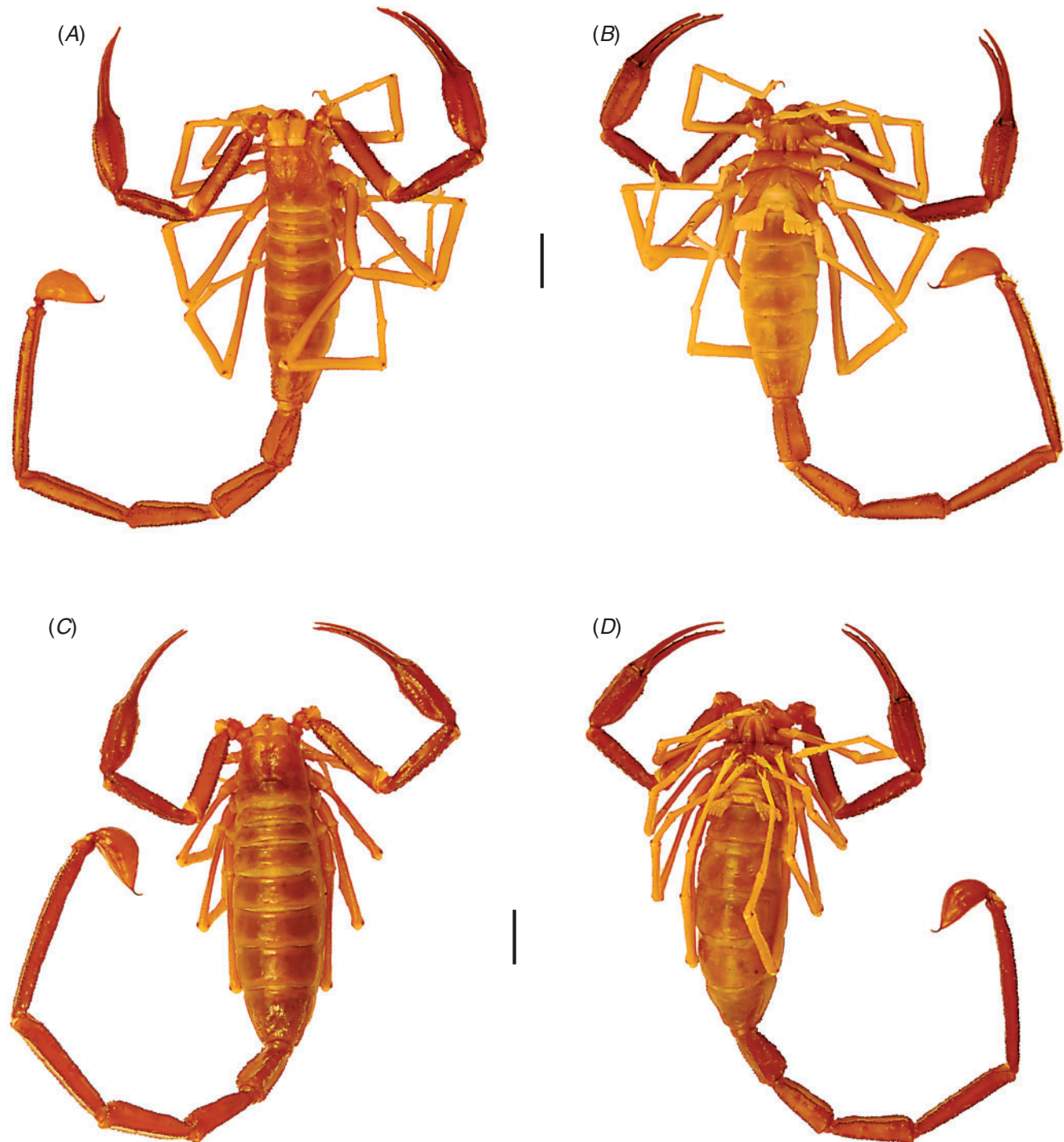


Fig. 2. *Alacran triquimera*, sp. nov., habitus. A, B. Holotype ♂ (CNAN-T0866). C, D. Paratype ♀ (CNAN-T0868). A, C. Dorsal view. B, D. Ventral view. Scale bars = 5 mm.

Humboldt, Villa de Leyva, Colombia (IAVH); Museum of Comparative Zoology, Harvard University, Cambridge, MA (MCZ); Muséum National d'Histoire Naturelle, Paris (MNHN); W. David Sissom Private Collection, Canyon, TX (WDS).

Observations were made using Nikon SMZ-800 and SMZ-1500 stereomicroscopes. Measurements (mm) follow Stahnke (1970) and were obtained with an ocular micrometer calibrated at 10×. Morphological terminology follows Stahnke (1970), except as follows: Hjelle (1990) and Sissom (1990) for pedipalp

segmentation; Jacob *et al.* (2004) for hemispermatophore; Francke (1977) for metasomal carination; Prendini (2000) for pedipalp carination; Prendini *et al.* (2010) for trichobothrial patterns; González-Santillán and Prendini (2013) for pedipalp chela finger dentition.

Digital images were taken under visible and ultraviolet light with a Nikon Coolpix S10 VR camera attached to a Nikon SMZ-800, and with a Nikon DS80 camera. The focal planes of image stacks were fused with CombineZM (Hadley 2008) and composite images edited with Adobe Photoshop.

Distribution maps were generated in ArcView 3.2 (ESRI) using the locality coordinates, a base map from the CONABIO (2011) digital database, and a digital elevation model from the CGIAR Consortium for Spatial Information (Jarvis *et al.* 2008).

Data matrix

The morphological data matrix of Prendini *et al.* (2010) was modified by adding *A. chamuco* and *A. triquimera*, sp. nov., omitting all except two species of *Typhlochactas* Mitchell, 1971, and adding three new characters. The resulting matrix comprised 182 qualitative characters of adult morphology scored for 10 terminal taxa (Table 1, Appendices 1, 2): the three species of *Alacran* representing the ingroup; four species representing the other typhlochactid genera, *Typhlochactas*, *Stygochactas* Vignoli & Prendini, 2009 and *Sotanochactas* Francke, 1986; and three species in the putatively most closely related genera, *Troglotayosicus* Lourenço, 1981 and *Superstitionia* Stahnke, 1940 (Prendini *et al.* 2010). All except *Troglotayosicus vachoni* Lourenço, 1981 were scored from freshly-collected or museum material (Appendix 1). The female holotype and only known specimen of *T. vachoni* was scored using the literature (Lourenço 1981, 2006). Four sex-specific characters contain question marks for taxa known from only one sex: *Stygochactas granulosus* (Sissom and Cokendolpher 1998); *T. vachoni*; *Typhlochactas sissomi* Francke *et al.* 2009. Two characters were polymorphic in *A. chamuco* and one in *A. triquimera*, sp. nov. Forty-six multistate characters were treated as unordered/nonadditive (Fitch 1971) in the analyses and 30 uninformative characters deactivated.

Cladistic analysis

Exact searches of the 151 informative characters were conducted in TNT (Goloboff *et al.* 2003a, 2003b, 2008), using the command *ienum*. Analyses were conducted with equal weighting and implied weighting, using six values of the concavity constant ($k=1, 3, 10, 30, 60$ and 100), to assess the effect of weighting against homoplasious characters. A preferred hypothesis was selected from among the alternative topologies recovered by the analysis of the dataset with equal weighting. The relative support for each node on the preferred hypothesis was calculated with Bremer support (Bremer 1994) and jackknife resampling (Farris *et al.* 1996). Bremer support was calculated in TNT by searching for suboptimal trees 30 steps longer, and holding 1000 trees per replication, using the script *bremer.run*. Jackknife support was estimated with heuristic searches of 1000 pseudoreplicates, using the commands *resample jak repl 1000*. Characters were optimised unambiguously on cladograms with

WinClada (Nixon 2002). Cladograms were edited with Adobe Illustrator C3.

Results

The analysis with equal weighting recovered a single most parsimonious tree (Fig. 3; Table 2) consistent with that obtained by Prendini *et al.* (2010). The monophyly of Typhlochactidae, Alacraninae, *Alacran*, Typhlochactinae Mitchell, 1971, *Typhlochactas*, and *Troglotayosicus* was confirmed and strongly supported by the same synapomorphies proposed in the previous analysis (e.g. 18 characters of trichobothria, and nine characters of pedipalp ornamentation). Relationships within *Alacran* were newly resolved as follows: (*A. chamuco* (*A. tartarus* + *A. triquimera*, sp. nov.)). *Alacran chamuco* was placed sister to a monophyletic group comprising *A. tartarus* and *A. triquimera*, sp. nov., supported by one synapomorphy, the presence of trichobothrium *esb*₃ on the retrolateral surface of the pedipalp patella. Analyses with implied weighting under six values of the concavity constant ($k=1, 3, 10, 30, 60$ and 100) recovered the same topology (Table 2).

Discussion

Geological history of the Sierra Madre del Sur

Alacran comprises three highly adapted (morphologically and presumably physiologically) troglobiotic scorpion species, inhabiting three isolated caves or cave-systems (Fig. 1). These caves occur in distinct sub-provinces of the Sierra Madre del Sur, i.e. Tres Quimeras in the Sierra Negra in Puebla (*A. triquimera*, sp. nov.), the Sistema Huautla in the Sierra Mazateca in Oaxaca (*A. tartarus*) and Te Cimutaá in the Sierra Juárez, also in Oaxaca (*A. chamuco*), raising the question of how this distribution originated.

The Sierra Madre del Sur has a complex geological history, resulting from the uplifting, faulting and over-trusting of Mesozoic rocks during the Laramide orogeny (Smith 2002). The region is dominated by limestones from the Orizaba formation (early Cretaceous–Tertiary), up to 5000 m thick and in places overlain by hard schists and other igneous/metamorphic rocks from the Jurassic. The limestones were deposited in a relatively shallow marine trough in the ancient proto-Gulf of Mexico, and that formation was subsequently raised by tectonic events in the Paleocene. As uplift occurred, erosion began on the land above sea level, leading to the current geomorphology of the southern Sierra Madre region.

The Sierra Mazateca is isolated from the Sierra de Juarez, to the south, by the Rio Santo Domingo Canyon, an impressive 1500 m deep gorge; and from the Sierra Negra, to the north, by the Rio Petlapa Canyon, an equally impressive 1000 m deep gorge. As the crow flies, the distance between Tres Quimeras and Sótano de San Agustín (the type locality of *A. tartarus*) is 18.8 km, the cave entrances are at 2720 m and 1440 m above sea level, respectively, and, in a straight line traverse, the lowest point between them, in the Rio Petlapa Canyon, is 340 m. Similarly, the distance between Te Cimutaá and Sótano de San Agustín is 50 km, the entrance to Te Cimutaá is at 1000 m and, in a straight line traverse, the lowest point between them, in the Rio Santo Domingo Canyon, is 244 m.

Table 1. Distribution of 182 morphological characters scored for phylogenetic analysis of the typhlochactid scorpion genus, *Alacran* Franché, 1982, and seven outgroup taxa

Taxa	Character									
	0000000000	0000000000	0000000000	0000000000	0000000000	0000000000	0000000000	0000000000	0000000000	0000000000
0000000000	1111111111	2222222222	3333333333	4444444444	5555555555	6666666666	7777777777	8888888888	9999999999	0123456789
0123456789	0123456789	0123456789	0123456789	0123456789	0123456789	0123456789	0123456789	0123456789	0123456789	0123456789
<i>Superstitionia donensis</i>	0010010000	1101200000	0101210100	0212201110	0112012111	1101010101	1010101020	2000000010	1001200011	1000111010
<i>Troglotayosicus humiculum</i>	1110000101	1100200000	0111000000	0212201111	0112122222	1100010111	1001100010	0100100010	0100221100	0100111010
<i>Troglotayosicus vachoni</i>	1110100201	0-00200000	10110100?0	0212201111	0112012111	1100010111	1001100010	0100100010	0100221100	0100111010
<i>Solanochactas ellioti</i>	1101101211	1010000111	1001101000	1212111111	1111101111	0100101000	0101001101	0000001101	0000211100	0111000001
<i>Stygochactas granulosus</i>	1001001211	1000200010	002000102	1001020001	0111011111	1100101000	0101001010	2000001010	1001100011	1001100001
<i>Typhlochactas rhodesi</i>	1100101211	1010111111	10010101?2	0212201111	0111012122	1100101000	0101001010	2000001010	0100211100	0100110001
<i>Typhlochactas sissonii</i>	11000101211	1011000011	1000101001	0112101111	0112011111	1100101000	0101001210	00000000101	0000211100	0100110001
<i>Alacran chanuco</i>	1100011211	1010200000	1101000001	1000020001	2000000000	0010101011	0111001221	2011A10012	0210221100	0110101110
<i>Alacran tartarus</i>	1100011211	1010200000	1101000001	1000020001	2000000000	0010101011	0111001221	2011A10012	2210221100	0110101110
<i>Alacran triquimera</i>	1100011211	1010300000	0101000001	1000020001	2000000000	0010101011	0111001221	2011A1012	2210221100	0110101110
Taxa	Character									
	0000000000	0000000000	0000000000	0000000000	0000000000	0000000000	0000000000	0000000000	0000000000	0000000000
0000000000	1111111111	2222222222	3333333333	4444444444	5555555555	6666666666	7777777777	8888888888	9999999999	0123456789
0123456789	0123456789	0123456789	0123456789	0123456789	0123456789	0123456789	0123456789	0123456789	0123456789	0123456789
<i>Superstitionia donensis</i>	1000111011	1100000010	00000100010	01000002120	00010000100	0100000021	1010011111	1111111111	1111111111	1111111111
<i>Troglotayosicus humiculum</i>	1000000000	11010000100	0201110012	0110011011	111-111101	0110110022	2011010000	00000022-1	10	
<i>Troglotayosicus vachoni</i>	1000000000	11010000100	0201110012	0110000???	00010000101	01101100???	2011010000	00000011011	10	
<i>Solanochactas ellioti</i>	0100000010	11010000101	1001001002	0202011111	111-111012	0011011120	0111000111	0101110000	01	
<i>Stygochactas granulosus</i>	0100000010	11010000100	2100100011	1010111100	1110110012	0111011110	2111101211	2211122101	01	
<i>Typhlochactas rhodesi</i>	0100000010	0011100100	2100020011	1011111110	1110111012	1210110110	0111101211	22111222-1	01	
<i>Typhlochactas sissonii</i>	0100000011	0100000100	2100020011	1011011100	1110111012	0111110110	?1111101211	2211121101	01	
<i>Alacran chanuco</i>	10111100020	1102011010	0110001110	010-010001	111-102012	001011012?	A10100010	1100100001	01	
<i>Alacran tartarus</i>	10111100020	1102011010	0110001110	010-010001	111-102012	0010100120	0110100010	1100100001	01	
<i>Alacran triquimera</i>	10111100020	1102011010	0010001110	010-010001	111-102012	0010100120	0110100010	1100100001	01	

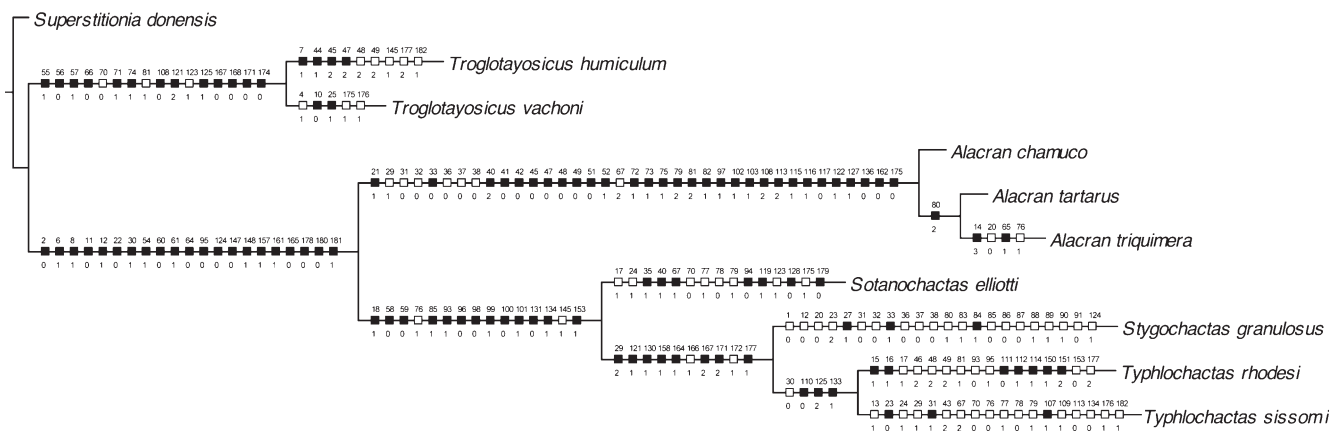


Fig. 3. Single most parsimonious tree (length: 282; Fit: 129.1; CI: 0.674; RI: 0.729) obtained from exact search of 151 informative morphological characters scored for three species of *Alacran* Francke, 1982 and seven outgroup taxa. Unambiguous synapomorphies optimized on branches: black squares indicate uniquely derived apomorphic states, white squares indicate parallel derivations of apomorphic states; numbers above squares indicate characters, numbers below indicate states. Jackknife values greater than 50% indicated above branches, Bremer support values below branches.

Table 2. Tree statistics for phylogenetic analysis of the typhlochactid scorpion genus, *Alacran* Francke, 1982, and seven outgroup taxa

Length, consistency index (CI), retention index (RI), Fit and adjusted homoplasy (AH) of most parsimonious trees obtained under equal weighting (EW) and implied weighting (IW), with six concavity values (*k*)

	MPTs	Length	CI	RI	Fit	AH
EW	1	284	0.676	0.730	130.10	—
IW: <i>k</i> = 1	1	284	0.676	0.730	109.67	42.33
IW: <i>k</i> = 3	1	284	0.676	0.730	130.1	21.9
IW: <i>k</i> = 10	1	284	0.676	0.730	143.8	8.2
IW: <i>k</i> = 30	1	284	0.676	0.730	149.05	2.95
IW: <i>k</i> = 60	1	284	0.676	0.730	150.5	1.5
IW: <i>k</i> = 100	1	284	0.676	0.730	151.09	0.91

Speleogenesis in the Sierra Madre del Sur

The process and history of cave formation (speleogenesis) is integral to understanding the biogeographical history of *Alacran*. Current views on the hydrogeology of karst aquifers are based on the triple porosity model, comprising matrix permeability, fracture permeability and conduit permeability (White 2012). Matrix permeability predominates in the early formation of the limestone deposits. Fracture permeability occurs after uplift, when parallel cracks and fissures develop between sedimentary layers along with perpendicular fractures connecting different layers through which water can flow and enlarge the spaces. Finally, conduit permeability occurs at or near the watertable level in the uplifted terrain as water flows downslope. This is also known as ‘hypogene speleogenesis’, defined as the formation of solution-enlarged permeability structures by water that recharges the cavernous zone from below, independent of recharge from the overlying or immediately adjacent surface (Klimchouk 2012).

The conduits formed by this phraeatic water vary in diameter depending on age and water flow, but are usually long and relatively uniform in size for considerable distances, with low

inclination following the dip of the watertable. Hypogene caves demonstrate remarkable similarity in their patterns, morphology, hydrostratigraphic occurrence, and current or inferred hydrogeological functioning, suggesting common hydrogeology (Klimchouk 2012).

Similar structure and geological history likewise suggests a common origin for the caves inhabited by the three species of *Alacran*. The long, slightly inclined conduit in the middle section of Tres Quimeras is hypogenic in origin, i.e. formed by phraeatic processes along the watertable level after the Orizaba formation was uplifted into the massive paleo-Sierra Madre del Sur (before surface erosion lead to its fragmentation into the three sub-provinces mentioned earlier). After considerable uplift, faulting and over-trusting, the hardened top layer (schists) of the paleo-Sierra Madre, with a long conduit hidden deep in the Orizaba limestones, was eroded, allowing percolating waters to reach the Orizaba formation. During the second phase of speleogenesis, gravitational water reached the deep, phraeatic conduit by seeping through cracks and minor faults. The geomorphology of the initial third of Tres Quimeras conforms to expectations from fracture permeability: the step-ladder structure develops as water seeps along a horizontal bedding plane, goes vertically through the bedding plane along a perpendicular crack, then flows gravitationally along the next bedding plane to the next perpendicular crack, and so on.

The Sistema Huautla is a larger, more complex version of Tres Quimeras: a long, deep conduit of phraeatic origin (many sections underwater await exploration), formed relatively early in the history of the Sierra Madre del Sur, coupled with a vadose system of infiltration and erosion in numerous dolinas and fracture permeability responsible for the twenty, very deep interconnected sotanos which converge in the older phraeatic conduit draining into the Santo Domingo River canyon 8–10 km away (Smith 2002).

At only 258 m long and 67 m deep (AMCS 2009a), Te Cimutaá is the outlier. Nevertheless, the geomorphology of this cave resembles the initial passages in Tres Quimeras, i.e. step-ladder

passages formed by fracture permeability, blocked from further exploration by a rock pile, raising the possibility that the blocked passage continues deeper until reaching a phraeatic conduit, as in the other caves. If so, a population of *A. chamuco* might exist in a deep, horizontal conduit near the watertable.

Vicariance and speciation of *Alacran*

Based on the geological history of the Sierra Madre del Sur and the likely similar speleogenesis of the Tres Quimeras, Sistema Huautla and Te Cimutaá, we propose a vicariance hypothesis to account for the disjunct distribution of the three species of *Alacran*, whereby an initially widespread, panmictic ancestral population speciated into three geographically isolated taxa following fragmentation of the southern Sierra Madre del Sur.

During the early history of the Sierra Madre del Sur, before erosion separated the three sub-provinces, an extensive phraeatic conduit system probably existed in the Orizaba formation. There are many examples of such extensive phraeatic systems in karstic formations, including Mexico, with more than fifteen caves at least 20 km long, and six caves more than 60 km long. In the Yucatan Peninsula, Sistema Sac Actun is 308 km long, and Ox Bel Ha is 242 km long. Thus, formation of an extensive system of interconnected conduits, hypogenic in origin, in the Orizaba formation is not unrealistic, and we hypothesise that it extended under the present Sierra Negra, Sierra Mazateca and Sierra de Juarez. We hypothesise further that the common ancestor of the three species of *Alacran* colonised and inhabited this extensive maze of phraeatic conduits where it was widely distributed in a fairly uniform cave environment, during which time it evolved many unique troglomorphies.

As the massive Sierra Madre del Sur continued to be uplifted, erosion began on the surface, leading to the formation of the proto-Rio Santo Domingo and proto-Rio Petlapa, along approximately the same courses they follow today, and separating the three sub-provinces of the Sierra Madre del Sur. Eventually, erosion along the Rio Santo Domingo and Rio Petlapa rivers cut through the limestone layers, reaching the depth of the deep, phraeatic conduit system and, once surpassing it, isolating the cave fragments and their associated scorpion populations in each mountain range. The isolated populations subsequently diverged, speciating into the three currently known species.

Support for this hypothesis exists in the Sierra Cuicateca, south of the Sierra Mazateca on the opposite side of the Rio Santo Domingo canyon, where several caves (e.g. Cueva de Peña Colorado, Sistema J2, Sistema Charco, Sistema Cheve; AMCS 2009b) conform geomorphologically to the concept, i.e. deep cave entrances with a meteoric speleogenesis leading into hypogenic conduits deep in the Orizaba formation. Cueva de Peña Colorado is essentially the end of a phraeatic conduit, mostly underwater, starting at a spring along the Rio Santo Domingo Canyon less than 2 km from the Huautla Resurgence. Indeed, Peña Colorado and the Huautla Resurgence are almost at the same elevation above sea level, on opposite sides of the Santo Domingo Canyon, suggesting they once formed a single,

continuous cavern. It is plausible that the stretch of the Rio Santo Domingo which now separates them was once a conduit. Likewise, a conduit that once connected Huautla and Te Cimutaá may now be part of the river channel which has eroded beyond recognition.

The Rio Santo Domingo canyon is deeper than the Rio Petlapa canyon, hence we hypothesise that the Sierra de Juarez became separated from the Sierra Mazateca + Sierra Negra massif first, isolating *A. chamuco* from the common ancestor of (*A. tartarus* + *A. triquimera*, sp. nov.) earlier, as reconstructed in the cladogram (Fig. 3). Subsequently, the Rio Petlapa disconnected the Sierra Negra from the Sierra Mazateca, leading to the isolation and divergence of *A. tartarus* from *A. triquimera*, sp. nov.

One remaining question is what happened to the *Alacran* populations in the caves of the Sierra Cuicateca? Presumably the Rio Santo Domingo separated the Sierra Cuicateca from the Sierra Mazateca more recently, so we would predict that *A. tartarus* or its sister species would occur there if indeed the phraeatic conduits of the Cueva de Peña Colorado and the Huautla Resurgence were once connected as we surmise. Extensive exploration in the caves of the Sierra Cuicateca, involving some of the same explorers who work on the Sierra Mazateca, has not produced any sightings or specimens of scorpions, however (W. Steele, pers. comm.). Whether they exist but inhabit unreachable sections of the caves, or have gone extinct remains a mystery.

Systematics

Family TYPHOLOCHACTIDAE Mitchell, 1971

Subfamily ALACRANINAE Vignoli & Prendini, 2009

Genus *Alacran* Francke, 1982

Key to the species of *Alacran* Francke, 1982

1. Pedipalp patella, ventral surface with 3–5 (usually 4) trichobothria, retro-lateral surface with 20–24 trichobothria; chela fixed finger, median denticle row comprising seven primary subrows flanked by six pro-lateral and six retrolateral denticles; movable finger, median denticle row comprising eight subrows flanked by seven pro-lateral and seven retrolateral denticles *Alacran triquimera*, sp. nov.
Pedipalp patella, ventral surface with 3 trichobothria, retrolateral surface with 19–21 trichobothria; chela fixed finger, median denticle row comprising six primary subrows flanked by five (rarely six) pro-lateral and five retrolateral denticles; movable finger, median denticle row comprising seven subrows flanked by six retrolateral denticles 2
2. Pedipalp chela, fixed finger, median denticle row comprising seven subrows flanked by six pro-lateral denticles. Telson length : carapace length ratio, 1.07; telson width : carapace length ratio, 0.47; telson depth : carapace length ratio, 0.43 *Alacran chamuco*
Pedipalp chela, fixed finger, median denticle row comprising seven subrows flanked by seven pro-lateral denticles. Telson length : carapace length ratio, 1.25; telson width : carapace length ratio, 0.58; telson depth : carapace length ratio, 0.57 *Alacran tartarus*

***Alacran tartarus* Francke, 1982**

(Figs 1, 3)

Alacran tartarus Francke, 1982: 51–57, 59, figs 1–17, 27, 32; table 1. *Alacran tartarus*: Lourenço & Francke, 1985: 5, table 1; Polis, 1990: 252; Nenilin & Fet, 1992: 28; Armas, 1994: 19, 21; Lourenço, 1994: 182, 183; Locket, 1995: 191; Kovářík, 1998: 142; Sissom & Cokendolpher, 1998: 289; Beutelspacher, 2000: 18, 20, 47, 51, 143, 151, map 20; Fet & Sissom, 2000: 496, 497; Lourenço & Sissom, 2000: 118; Sissom, 2000: 498; Soleglad & Sissom, 2001: fig. 40; Volschenk *et al.* 2001: 161; Soleglad & Fet, 2003a: 6, figs 8, 10; Soleglad & Fet, 2003b: 8, 76; Prendini & Wheeler, 2005: 454, 469, table 5, figs. 12, 13; Graham & Fet, 2006: 7; Volschenk & Prendini, 2008: 236, table 1; Kamenz & Prendini, 2008: 10, 44, table 2; Sissom & Reddell, 2009: 22–23; Vignoli & Prendini, 2009: 9, 18, 28, 29, 31, 34, 35, figs 1, 3E, F, 4, 5A, 6A, B, 7A, 9A, B, 10A–D, 11, 13–16, table 2, 5, 6; Francke, 2009: 47, 48, 55, fig. 6, 11, 13, 15, 17, 19, table 2; Prendini *et al.* 2010: 2, 4, 18, 21, figs 1, 3C, D, 4, 5A, 6A, 7A, 8A, H, 9, 10, tables 1, 2.

Material examined

Mexico: Oaxaca: Municipio de San Miguel: Sótano de San Agustín [18°06'23"N 96°47'53"W, 720 m], San Agustín, 5 km SE Huautla de Jiménez, 1979 San Agustín Expedition members of the Huautla Project, Spring 1979, holotype ♀, 1 juv. ♂ paratype (AMNH); Sótano de San Agustín Section, Sistema Huautla, A.G. Grubbs, J.H. Smith & F. Holliday, v.1985, 2 ♀ (WDS); Sótano Li Nita [18°08'51"N 96°47'56"W, 812 m], San Agustín, 5 km SE Huautla de Jiménez, B. Steele & S. Zeman, 1980 Río Iglesia Expedition, 29.iii.1980, paratype ♂ (AMNH), M. Minton, L. Wilk & R. Simmons, 1.iv.1981, 1 ♀ (AMNH); Sótano Li Nita [18°08'51"N 96°47'56"W], San Agustín, 5 km SE Huautla de Jiménez, White Room Lead, 871 m, M. Minton, 22.iii.1981, 1 juv. ♀ (AMNH); Sótano Agua de Carrizo [18°08'16"N 96°47'39"W, 760 m], 5 km ESE Huautla de Jiménez, A.G. Grubbs, B. Stone, J. Smith, T. Johnson & M. McEachern, 23.v.1978, 1 juv. ♀ paratype (AMNH); Cueva del Escorpión, San Miguel Dolina, 5 km SE Huautla de Jiménez, R. Jameson & P. Mothes, i.1978, paratype ♀ (MNHN); Cueva del Escorpión, 18°06'23"N 96°47'53"W, 1561 m, A. Gluesenkamp, P. Sprouse & C. Savvas, 18.ix.2004, 1 ♂ (AMNH), leg (AMCC [LP 3499]).

Diagnosis:

Alacran tartarus may be distinguished from the other two species of *Alacran* as follows. The median denticle row of the fixed finger of the pedipalp chela comprises six primary subrows flanked by five (rarely six) prolateral and five retrolateral denticles in *A. tartarus*, compared with seven subrows flanked by seven prolateral and six retrolateral denticles in *A. triquimera*, sp. nov. The median denticle row of the movable finger comprises seven primary subrows flanked by seven prolateral and six retrolateral denticles in *A. tartarus*, compared with eight subrows flanked by seven prolateral and seven retrolateral denticles in *A. triquimera*, sp. nov. The ventral surface of the pedipalp patella possesses 3 trichobothria and the retrolateral surface, 19–21 in *A. tartarus* compared with 3–5 (usually 4) and 22–24, respectively, in *A. triquimera*, sp. nov. The ratio of telson length:carapace length is greater in *A. tartarus* (1.25) than in *A. chamuco* (1.07).

Distribution

Endemic to the caves of the Sistema Huautla in the state of Oaxaca (Fig. 1), south-eastern Mexico. This cave system in the heart of the Sierra Mazateca comprises twenty entrances, with

many additional springs and unexplored entrances and passages. An exploration in 2002 covered 62 099 m of passage to a depth of –1475 m. The Huautla Resurgence, on the Rio Santo Domingo Canyon is ~8.2 km south of the entrance to Sótano de San Agustín, the type locality of *A. tartarus*, and 10.2 km from the entrance to Nita Nauta, 300 m above sea level, 1760 m lower than the entrance to Nita Nauta (Steel and White, 2012).

Ecology

Like other species of the genus, *A. tartarus* is an obligate troglobiont. It has been collected in four different caves in the Sistema Huautla (Cueva del Escorpión, Sótano Agua de Carrizo, Sótano de San Agustín and Sótano Li Nita), at depths ranging from –912 m to –60 m below the entrance, the deepest records at which a scorpion has been found, with most sightings and collections at greater depths (W. Steele, pers. comm.). This species is predominantly found near water and has been observed numerous times walking underwater, as much as 6 m deep in pools near the bottom of the cave system as the sumps were explored by scuba divers (W. Steele and J. Smith, pers. comm.).

***Alacran chamuco* Francke, 2009**

(Figs 1, 3)

Alacran chamuco Francke, 2009: 46–55, figs 1–5, 7–9, 12, 14, 16, 18, 20, tables 1, 2.

Alacran sp.: Vignoli & Prendini, 2009: 4, 8, 35, fig. 1A, table 2.

Material examined:

Mexico: Oaxaca: Municipio de Valle Nacional: Te Cimutaá (cave) (NAD 27 777899 1987404) [17°54.241'N 96°22.626'W], 944 m, 25.iv.2008, P. Bryant, holotype ♀ (CNAN-T0401), leg (AMCC [LP 8571]).

Diagnosis:

Alacran chamuco may be distinguished from the other two species of *Alacran* as follows. The median denticle row of the fixed finger of the pedipalp chela comprises six primary subrows flanked by five prolateral and five retrolateral denticles in *A. chamuco*, compared with seven subrows flanked by six prolateral and six retrolateral denticles in *A. triquimera*, sp. nov., and six primary subrows flanked by six prolateral and five retrolateral denticles in *A. tartarus*. The median denticle row of the movable finger comprises seven primary subrows flanked by six prolateral and six retrolateral denticles in *A. chamuco*, compared with eight subrows flanked by seven prolateral and seven retrolateral denticles in *A. triquimera*, sp. nov. The ventral surface of the pedipalp patella possesses 3 trichobothria and the retrolateral surface, 20 or 21 in *A. chamuco* compared with 3–5 (usually 4) and 20–24, respectively, in *A. triquimera*, sp. nov. The ratio of telson length:carapace length is less in *A. chamuco* (1.07) than in *A. tartarus* (1.25).

Supplementary description:

The following description and meristic data (Tables 3, 4) for the holotype ♀ supplements the original description by Francke (2009). Details as for *A. triquimera*, sp. nov., except where noted.

Table 3. Meristic data for two species of the typhlochactid scorpion genus, *Alacran* Francke, 1982: *Alacran chamuco* Francke, 2009 (triangle); *Alacran triquimera*, sp. nov. Measurements (mm) follow Prendini *et al.* (2003)

		<i>Alacran chamuco</i>						<i>Alacran triquimera</i> , sp. nov.								
Type:		Holotype adult ♀	Holo. ad. ♂	Para. ad. ♂	Para. ad. ♂	Para. ad. ♂	Para. ad. ♀	Para. ad. ♀	Para. ad. ♀	Para. ad. ♀	Para. subad. ♀	Para. subad. ♀	Para. juv. ♀			
Type:																
Stage:																
Sex:																
Total Length		63.2	62.3	65.8	61	60.7	61.8	63.8	39.2	67.3	73.6	56.5	53.6	43.1		
Carapace	length	5.3	4.8	5	4.7	4.6	5.2	5.1	5.2	5.1	5.7	4.6	4.4	3.9		
	anterior width	5	4.4	4.5	4.2	4.3	4	4.7	4.5	4.4	5	4	3.5	3.2		
	posterior width	5.5	5	5.4	5	5	4.9	5.6	5.9	5.6	6	4.8	4.5	3.7		
Mesosoma length		15	13.1	15.2	12.4	13.6	14	14.5	16.5	17.3	18.3	13.6	13.7	10.8		
Metasoma length		37.2	38.8	39.7	38.2	36.6	36.8	38.6	17.5	39.3	43.2	34.1	30.9	24.8		
Metasoma I	length	4.5	4.6	4.7	4.5	4.4	4.6	4.6	4.8	4.8	5.2	4.2	3.8	3.1		
	max width	2.5	2.2	2.4	2.2	2.3	2.4	2.3	2.7	2.6	2.7	2.2	2	1.8		
	max height	2.1	2	2.1	2	1.9	2	2.1	2.3	2.2	2.4	2	1.6	1.6		
Metasoma II	length	5.3	5.5	5.6	5.4	5.4	5.4	5.6	5.8	5.6	5.9	5	4.3	3.6		
	max width	2.2	1.9	2.4	1.9	2.1	2.2	2	2.5	2.5	2.5	2.2	1.9	1.7		
	max height	1.9	1.9	2	1.8	1.8	1.8	2	2	2	2.2	1.8	1.5	1.4		
Metasoma III	length	6.2	6.5	6.5	6.5	6.2	6.4	6.4	6.9	6.7	7.3	5.8	5.2	4.1		
	max width	2	1.8	2.2	1.8	2	2.1	2	2.4	2.3	2.4	2	1.8	1.6		
	max height	1.8	1.8	1.8	1.6	1.6	1.7	1.9	1.9	1.8	2	1.7	1.4	1.2		
Metasoma IV	length	8.6	8.9	9.3	9	8.9	8.6	8.9	—	9	9.9	8	7.3	5.6		
	max width	1.6	1.5	1.7	1.6	1.5	1.7	1.6	—	1.7	1.8	1.4	1.4	1.3		
	max height	1.4	1.4	1.4	1.3	1.3	1.3	1.6	—	1.6	1.7	1.4	1.2	1		
Metasoma V	length	12.6	13.3	13.6	12.8	11.7	11.8	13.1	—	13.2	14.9	11.1	10.3	8.4		
	max width	1.3	1.2	1.3	1.2	1.3	1.3	1.2	—	1.4	1.5	1.2	1.2	1		
	max height	1	0.9	0.9	0.9	1	1	1.1	—	1.1	1	0.7	0.9	0.7		
Telson	length	5.7	5.6	5.9	5.7	5.9	5.8	5.6	—	5.6	6.4	4.2	4.6	3.6		
	aculeus length	0.7	0.8	0.9	0.9	1	0.9	0.8	—	0.9	1	0	0.9	0.6		
	vesicle length	5	4.8	5	4.8	4.9	4.9	4.8	—	4.7	5.4	4.2	3.7	3		
	width	2.5	2.5	2.7	2.5	2.5	2.5	2.4	—	2.5	3.1	2.3	2	1.6		
	height	2.3	2.5	2.7	2.4	2.4	2.5	2.4	—	2.2	2.6	2	1.8	1.4		
Pedipalp length		28.2	27.1	28.3	26.8	27.2	27.8	26.4	28.9	27.9	31.9	25	23.2	20		
Femur	length	7.9	7.8	7.5	7.6	7.4	7.7	7.4	8	7.5	8.5	6.8	6.3	5.5		
	width	1.8	1.4	1.5	1.5	1.4	1.4	1.6	1.6	1.5	1.6	1.4	1.1	1		
	height	1	0.6	0.9	0.7	0.7	0.7	0.7	0.9	0.7	0.9	1	0.8	0.6		
Patella	length	7.2	6.7	7.3	7	7	7.4	7.3	7.5	7.2	8.1	6.5	6	5.1		
	width	1.9	1.4	1.5	1.4	1.4	1.5	1.5	1.6	1.7	1.4	1.6	1.3	1.2		
	height	1.8	1.1	1.4	1.2	1.3	1.4	1.2	1.4	1.2	1.4	1.5	1.2	1.1		
Chela	length	13.1	12.6	13.5	12.2	12.8	12.7	11.7	13.4	13.2	15.3	11.7	10.9	9.4		
	max width	2.8	2.4	2.4	2.3	2.2	2.4	2.5	2.4	2.2	2.5	2	2.9	1.5		
	max height	3.2	2.9	2.8	2.7	2.8	3	3.1	3	2.9	3.1	2.7	2.2	2		
	movable finger length	8.1	7.5	7.9	7.3	7.5	7.5	7.5	7.9	7.8	9.1	6.9	6.5	5.5		
	fixed finger length	6.8	6.4	6.2	6.3	6.5	6.5	6.5	6.6	6.3	7.4	5.5	5.3	4.2		

Carapace: anterior margin with six microsetae.

Pedipalps: fixed finger, median denticle row comprising six oblique primary subrows flanked by five prolateral and five retrolateral denticles, equal in size. Movable finger, median denticle row comprising seven oblique primary subrows flanked by six prolateral and six retrolateral denticles. Patella with 26/27 (sinistral/dextral) trichobothria, including 7/8 accessory (*et*_{4–6}, *est*₂, *em*_{3–5}, *esb*₃): three ventral (*v*_{1–3}); 20/21 retrolateral (*et*_{1–6}, *est*_{1, 2}, *em*_{1–5}, *esb*_{1–3}, *eb*_{1–5}); two dorsal (*d*_{1, 2}); one prolateral (*i*).

Genital operculum: sclerites (♀) fused, but loosely connected by membrane along entire length of suture.

Pectines: tooth count, 5/5 (♀).

Sternites: respiratory spiracles (stigmata) small, rounded, situated posterolaterally.

Distribution

Known only from the type locality, Te Cimutaá (cave) in the state of Oaxaca (Fig. 1), south-eastern Mexico. Te Cimutaá is

Table 4. Variation in trichobothrial counts on the sinistral and dextral (l/r) pedipalps of three species in the typhlochactid scorpion genus, *Alacran* Francke, 1982: *Alacran chamuco* Francke, 2009, *Alacran triquimera*, sp. nov. and *Alacran tartarus* Francke, 1982

Specimens deposited in the following collections: American Museum of Natural History (AMNH); Colección Nacional de Arácnidos, Instituto de Biología, Universidad Nacional Autónoma de México, Mexico City (CNAN); Muséum National d'Histoire Naturelle, Paris (MNHN)

Species	Type	Sex	Collection	Patella e (l/r)	Patella v (l/r)	Patella total (l/r)	Pedipalp total (l/r)
<i>A. chamuco</i>	Holotype	♀	CNAN-T0401	21/20	3/3	27/26	56/55
<i>A. tartarus</i>	Paratype	♂	AMNH	21/21	3/3	27/27	56/56
		♂	AMNH	21/21	3/3	27/27	56/56
	Holotype	♀	AMNH	21/21	3/3	27/27	56/56
	Paratype	♀	MNHN RS 7439	21/21	3/3	27/27	56/56
		♀	AMNH	20/21	3/3	26/27	55/56
		♀	WDS	21/21	3/3	27/27	56/56
		♀	WDS	19/21	3/3	25/27	54/56
	Paratype	juv. ♂	AMNH	21/21	3/3	27/27	56/56
	Paratype	juv. ♀	AMNH	21/21	3/3	27/27	56/56
		juv. ♀	AMNH	21/20	3/3	27/26	56/55
<i>A. triquimera</i>	Holotype	♂	CNAN-T0866	21/21	4/3	28/27	57/56
	Paratype	♂	CNAN-T0867	21/22	4/4	28/29	58/58
	Paratype	♂	CNAN-T0869	22/22	4/4	29/29	58/58
	Paratype	♂	AMNH	22/22	4/4	29/29	58/58
	Paratype	♂	CNAN-T0869	21/21	4/4	28/28	57/57
	Paratype	♀	CNAN-T0868	22/24	5/4	30/31	59/60
	Paratype	♀	CNAN-T0870	23/22	4/4	30/29	59/58
	Paratype	♀	AMNH	20/22	4/4	27/29	56/58
	Paratype	♀	CNAN-T0870	22/22	4/4	29/29	58/58
	Paratype	subad. ♀	CNAN-T0868	22/21	4/5	29/29	58/58
	Paratype	subad. ♀	CNAN-T0869	22/22	4/4	29/29	58/58
	Paratype	juv. ♀	AMNH	21/20	4/4	28/27	57/56

situated in the speleologically unexplored Sierra de Juarez, south of the Rio Santo Domingo Canyon near Valle Nacional. The entrance is 1000 m above sea level, and the cave is 258 m long and 67 m deep. Slightly more than half its length slopes gently at ~45° and the final half is steeper at ~75–80°. The cave ends blindly in a rock collapse that blocks further exploration (AMCS 2009a). Little else is known about the type locality and habitat of the single known specimen of *A. chamuco*. The type locality of *A. tartarus* (Cueva del Escorpión) is also a relatively short, steep cave that is unconnected to the other 20 entrances of the Sistema Huautla; dyes poured into a nearby spring were recovered deep in Sótano de San Agustín, establishing a hydrogeological connection (Smith 2002). Undoubtedly, there are cracks and narrow fissures through which scorpions from the depths of San Agustín can reach the relatively shallow Cueva del Escorpión. Perhaps there is also a deep, wet passage below the rock-collapse in Te Cimutaá where the population of *A. chamuco* normally resides.

Ecology

Like other species of the genus, *A. chamuco* is an obligate troglobiont.

Alacran triquimera, sp. nov.

(Figs 1–8)

urn:lsid:zoobank.org:pub:D4EE0BBA-F451-4315-ABBE-A6679E313E5D

Material examined

Mexico: Puebla: Municipio de Tlacotepec de Díaz: Cueva las Tres Quimeras (NAD 27 UTM zone 14: 727682 × 2025892; 18.3116°N 96.8458°W, 1440 m), ~530 m, 1.iv.2009, B. Shade, holotype ♂ (CNAN-T0866), paratype ♂ (AMCC [LP 9983]), 2.iv.2009, E. Légaré & J.F. Levis, paratype ♀ (CNAN-T0867), 10.iv.2009, B. Shade, paratype ♀, 1 subadult ♀ paratype (CNAN-T0868); ~500 m, 10 cm from water, 4.ii.2009, J.F. Levis & E. Légaré, 1 ♀ paratypes (CNAN-T0869); ~600 to ~550 m, 4.vii.2009, J.F. Levis & E. Légaré, 1 paratype ♂, 1 paratype ♀, 1 juv. ♀ paratype (AMNH); ~550 m, not in water, 6.iv.2009, 2 ♂ paratypes, 1 subad. ♀ paratype (CNAN-T0870).

Diagnosis

Alacran triquimera, sp. nov. may be distinguished from the other two species of *Alacran* as follows. The ventral surface of the pedipalp patella possesses 3–5 (usually 4) trichobothria and the retrolateral surface, 20–24 in *A. triquimera*, sp. nov. compared with 3 and 19–21, respectively, in *A. tartarus*, and 3 and 20 or 21, respectively, in *A. chamuco*. The median denticle row of the fixed

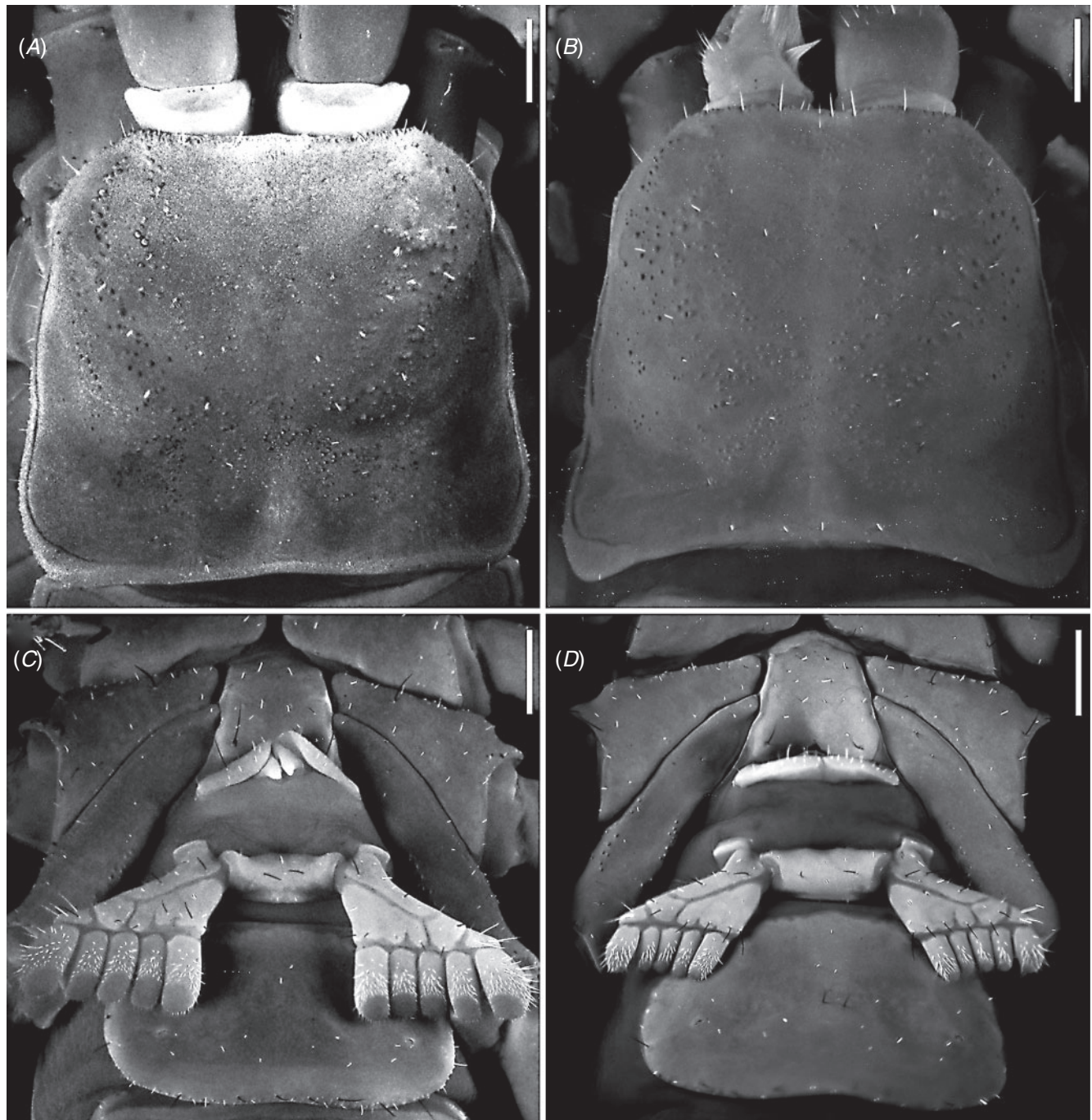


Fig. 4. *Alacran triquimera*, sp. nov., carapace, dorsal view (A, B), sternum, genital operculum and pectines, ventral view (C, D). A, C, Paratype ♂ (CNAN-T0870). B, D, Paratype ♀ (CNAN-T0868). Scale bars = 1 mm.

finger of the pedipalp chela comprises seven primary subrows flanked by six prolateral and six retrolateral denticles in *A. triquimera*, sp. nov., compared with six subrows flanked by five prolateral and five retrolateral denticles in *A. chamuco* and five (rarely six) prolateral and five retrolateral denticles in *A. tartarus*. The median denticle row of the movable finger comprises eight subrows flanked by seven prolateral and seven retrolateral denticles in *A. triquimera*, sp. nov.,

compared with seven subrows flanked by six prolateral and six retrolateral denticles in *A. chamuco* and seven subrows flanked by six (rarely seven) prolateral and six retrolateral in *A. tartarus*.

Description:

Based on holotype ♂ (Fig. 2A, B) and paratype ♀ (Fig. 2C, D).

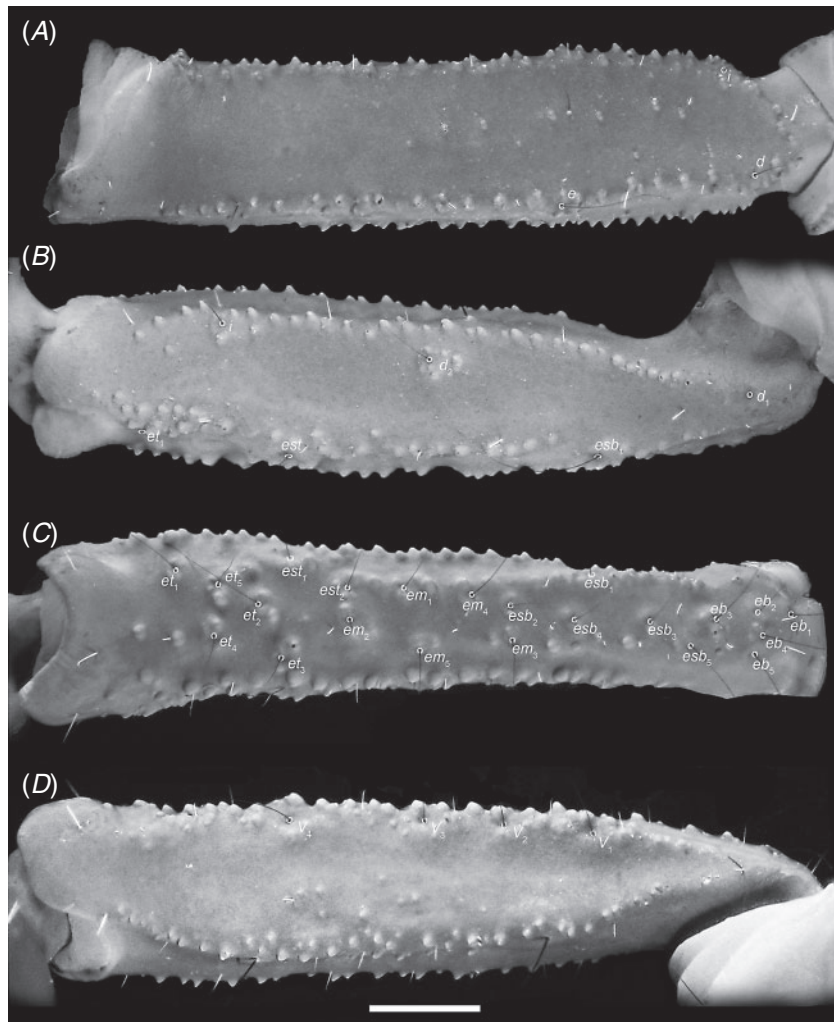


Fig. 5. *Alacran triquimera*, sp. nov., paratype ♂ (CNAN-T0870), sinistral pedipalp femur (*A*) and patella (*B–D*). *A, B*, Dorsal view. *C*, Retrolateral view. *D*, Ventral view. Scale bar = 1 mm.

Color: adult, carapace, pedipalp femur, tergites and metasomal segments amber to pale yellow brown, with darker carinae. Chelicerae pale yellow; teeth dark. Pedipalp patella and chela, orange brown; chela fingers slightly darker, reddish brown. Legs and sternites, pale yellow. Pectines, pale yellow to cream. Telson yellowish orange, aculeus dark.

Chelicerae: manus, dorsal and ventral surfaces smooth; dorsal surface with two distal microsetae and one medial microseta; ventral surface with short brush-like macrosetae becoming longer on fixed finger. Fixed finger with four teeth (distal, subdistal, median and basal); median and basal teeth fused into bicuspid; distal tooth largest, subdistal smaller than distal but larger than median and basal; median and basal teeth equal. Movable finger, prolateral distal and retrolateral distal teeth opposable, prolateral distal tooth completely overlapping retrolateral distal tooth in dorsal view; dorsal margin with five teeth (prolateral distal, two subdistal, median and basal); prolateral distal tooth largest, other teeth equal in size; ventral surface with serrula, extending less than half length of finger, completely covered by long, dense macrosetae.

Carapace: length slightly greater than anterior width (Table 3). Anterior margin sublinear, without median projection (epistome); with 5–6 microsetae (Fig. 4*A, B*). Posterior margin concave; asetose. Median and lateral ocelli absent. Median longitudinal sulcus obsolete; posterolateral sulci shallow; posterior transverse sulcus deep. Surface acarinate, with scattered subspiniform granules.

Pedipalps: femur dorsal retrolateral, dorsal prolateral, ventral prolateral, ventral retrolateral, and retrolateral median carinae distinct, comprising discontinuous rounded to spiniform granules (Fig. 5*A*); retrolateral median and ventral retrolateral carinae less developed, comprising fewer granules. Dorsal surface smooth, with few granules proximally to medially; retrolateral surface granular; ventral surface with few granules proximally and short row of granules distally; prolateral surface with few granules proximally, smooth distally. Patella dorsal retrolateral, dorsal prolateral, ventral retrolateral, and ventral prolateral carinae distinct, granular; prolateral median and retrolateral median carinae obsolete (Fig. 5*B–D*). Dorsal surface slightly concave and smooth except for two small granular areas surrounding



Fig. 6. *Alacran triquimera*, sp. nov., paratype ♂ (CNAN-T0870), sinistral pedipalp chela. A, Dorsal view. B, Retrodorsal view. Scale bar = 1 mm.

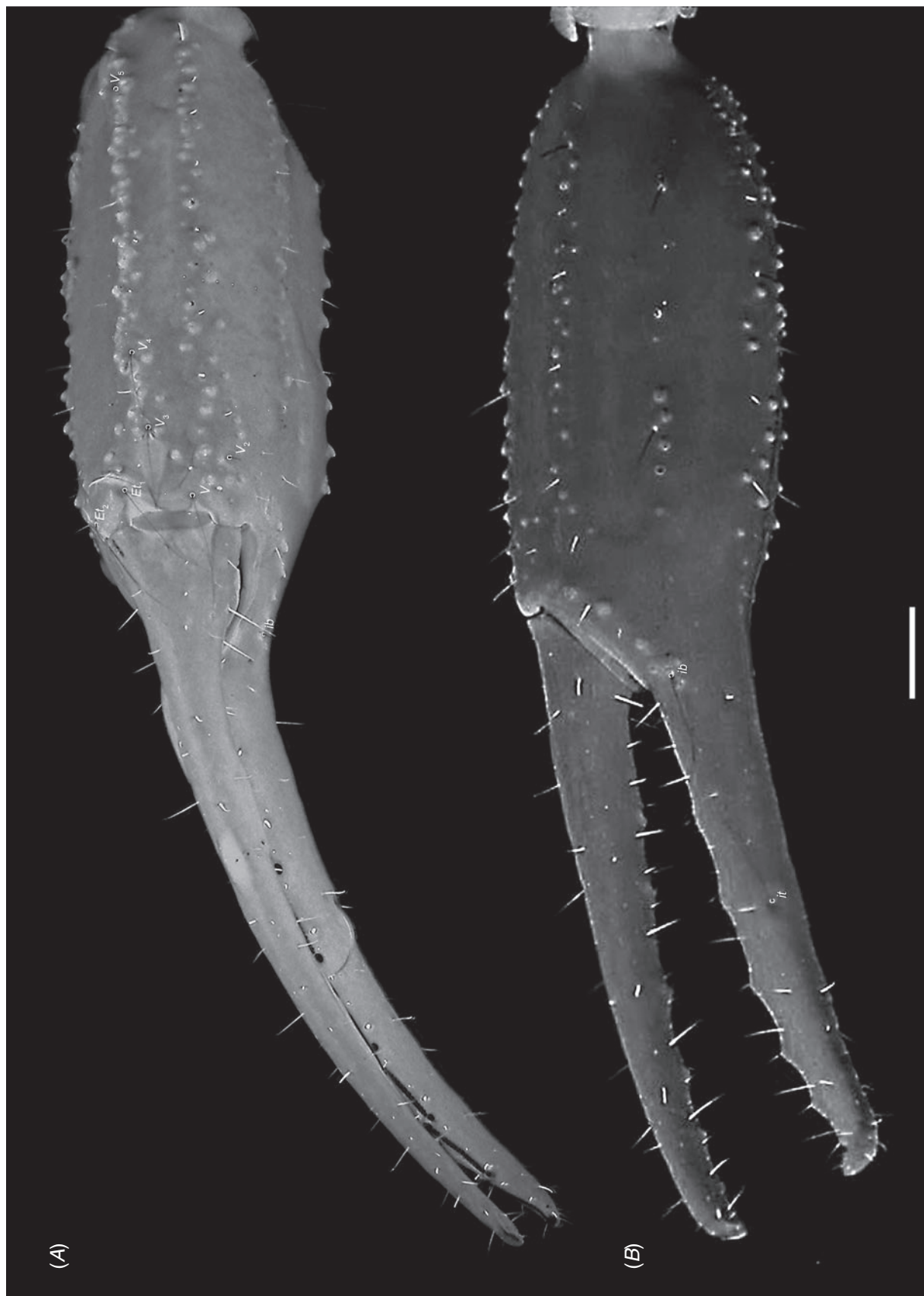


Fig. 7. *Alacran triquimera*, sp. nov., paratype ♂ (CNAN-T0870), simstral pedipalp chela. *A*, Ventral view. *B*, Proventral view. Scale bar = 1 mm.



Fig. 8. *Alacran triquimera*, sp. nov., paratype ♂ (CNAN-T0870), sinistral hemispermatophore. *A*, Ectal view. *B*, Capsule area, dorsal view. *C*, Capsule area, ventral view. Scale bars = 1 mm.

trichobothria d_2 and i ; retrolateral surface with several large granules, close to trichobothria; ventral surface smooth. Chela long, with relatively large, swollen manus (Figs 6, 7). Dorsal median, dorsal secondary, digital, ventral retrolateral, ventral median and ventral prolateral carinae distinct, similar, each comprising row of granules; retrolateral secondary carina distinct but weaker, comprising fewer, smaller granules; dorsal prolateral and prolateral median carinae comprising few isolated granules between dorsal median and ventral median carinae. Manus, intercarinal surfaces smooth; prolateral surface with prominent, isolated granule near movable finger condyle and row of prominent, isolated granules from base of movable finger to base of fixed finger; fixed finger smooth. Fixed finger, median denticle row comprising seven oblique primary subrows flanked by six prolateral and six retrolateral denticles, equal in size. Movable finger, median denticle row comprising eight oblique primary subrows flanked by seven prolateral and seven retrolateral denticles. Fixed and movable fingers, terminal denticles considerably larger than preceding denticles, hook-like, interlocking unevenly when fingers closed. Femur with three trichobothria (Fig. 5A): one retrolateral (e), one dorsal (d), one prolateral (i). Patella with 27–31 trichobothria

(Fig. 5B–D; Table 4), including eight (rarely nine, ten, eleven, twelve or thirteen) accessory ($et_{4–6}$, est_2 , $em_{3–6}$, $esb_{3–5}$, $v_{4, 5}$): 3–5 (usually 4) ventral ($v_{1–5}$); 20–24 retrolateral ($et_{1–6}$, $est_{1, 2}$, $em_{1–6}$, $esb_{1–5}$, $eb_{1–5}$); two dorsal ($d_{1, 2}$); one prolateral (i). Chela with 29 trichobothria (Figs 6, 7): three accessory (em , Em , V_5): 18 on manus, five ventral ($V_{1–5}$), 11 retrolateral ($Et_{1–5}$, Est , Esb , Em , $Eb_{1–3}$), two dorsal (Dt , Db); 11 on fixed finger, five retrolateral (et , est , em , esb , eb), four dorsal (dt , dst , dsb , db), two prolateral (it , ib). All trichobothrial areolae small, similar in diameter, trichobothrial setae similar in length (none ‘petite’).

Legs: femur and patella elongated, patella slightly shorter than femur. Femur laterally compressed; unicarinate; dorsal and ventral surfaces separated by row of distinct granules; surfaces with few macrosetae. Patella less compressed than femur; dorsal surface smooth; ventral edge granular; surfaces sparsely setose. Basitarsi prolateral, retrolateral and proventral surfaces with macrosetae, similar in number on I–III, fewer on IV; I–IV, each with large prolateral pedal spur; I and II, proventral surface without spinules. Telotarsi, dorsal median lobe with one large microseta; ventral surface without spinules and with at least 8–10 ventral submedian pairs of thin, acuminate macrosetae; unguis well developed, curved, equal in length; dactyl large, prominent.

Tergites: pretergites, surfaces smooth. Post-tergites I and II, surfaces smooth; III–VII, surfaces with scattered granules posteriorly; VII, lateral margins with small spiniform granules in posterior three-quarters, large sparse granules medially; I–VI, acarinate; VII, dorsal submedian carinae vestigial, reduced to few posterior granules, dorsal lateral carinae distinct, comprising few scattered granules (Fig. 2).

Sternum: posterior width greater than length (Fig. 4C, D); apex rounded; lateral margins converging anteriorly; lateral lobes flat; posterior depression shallow. Surface with two macrosetae and several microsetae.

Genital operculum: sclerites (♂) completely divided; genital papillae protruding distinctly beyond posterior edges (Fig. 4C). Sclerites (♀) fused, but loosely connected by membrane along entire length of suture. Surfaces covered by microsetae (Fig. 4D).

Pectines: pectinal plate, surface with several macrosetae. Lamella comprising three (♂) or four (♀) segments (Fig. 4C, D); surfaces with 8–10 macrosetae and several microsetae. Tooth count, 5/5 (♂) or 5–6/5 (♀); teeth elongated, 0.77 times longer in male than female; proximal and distal teeth slightly larger; surfaces covered with microsetae.

Sternites: sternites III–VI, anterior margins sublinear, posterior margins slightly concave, with few macrosetae; lateral and posterior margins with very small granules; VII, surfaces more granular, especially in posterior half, with pair of weakly developed ventrolateral carinae. Respiratory spiracles (stigmata) small, ellipsoid, situated posterolaterally.

Metasoma: segments elongated, length greater than width, progressively increasing in length, decreasing in width (Table 3); segment V longer than carapace. Dorsal submedian carinae, segments I–IV, distinct, granular; V, absent. Dorsal lateral carinae, segments I–III, weakly developed, sparsely granular; IV, absent; V, distinct, granular. Median lateral carinae, segments I and II, distinct, granular, incomplete; III–V, absent. Ventral lateral carinae, segments I–V, distinct, granular, complete. Ventral submedian carinae, segments I–IV,

and ventral median carina, segment V, absent. Anal arch smooth dorsally, granular and setose ventrally. Intercarinal surfaces smooth except dorsal surfaces, segments IV and V, sparsely granular. Lateral and ventral intercarinal surfaces with few microsetae, increasing in number from segments I–V.

Telson: vesicle globose, slightly compressed laterally; anterodorsal lateral lobes absent; surface smooth with few, small granules along anterodorsal margin; few short macrosetae anteriorly; short microsetae ventrally and near base of aculeus. Aculeus very short, arising abruptly from vesicle, slightly curved, surface smooth.

Hemispermatophore: lamelliform, basal portion narrow (Fig. 8); capsular region with large, sclerotised lobe; spiniform processes absent. Total length, 9.4 mm; lamella length, 6.4 mm; capsule width, 0.9 mm.

Ontogenetic variation: subadults and juveniles differ from adults as follows. Colour pale yellowish cream except for cheliceral teeth, pedipalp chela denticle rows, unguis and aculeus, brown. Carapace, anterior margin with median projection (epistome) well developed in subadult to obsolete in juvenile. Pedipalpal and metasomal carination mostly absent in juvenile to weakly developed in subadult. Surface granulation less developed in subadult and juvenile. Telson less globose and more setose in juvenile.

Sexual dimorphism: adult male similar to adult female, except for slightly more pronounced carination and granulation, completely divided genital operculum, presence of genital papillae and slightly larger pectinal teeth.

Distribution

Known only from the type locality, Tres Quimeras cave, in the state of Puebla (Fig. 1), south-eastern Mexico. Tres Quimeras, located in the Sierra Negra, near the town of Tlacotepec de Díaz, has three precipitous entrances ~20 m apart hence the name. The entrances, located at 1440 m above sea level, join at approximately –80 m, followed by a cascade of drops and passages ~1300 m long, slowly descending to about –420 m, where the cave becomes a 2000 m long, slowly descending passage (where all known specimens of *A. triquimera*, sp. nov. were collected). Finally, a more inclined descent, 1200 m long, opens on the wall of the Rio Petlapa Canyon, some 4.5 km away and 513 m lower than the entrances (B. Shade, pers. comm.).

Ecology

Like other species of the genus, *A. triquimera* is an obligate troglobiont, inhabiting some of the world's deepest caves at depths of –420 m to –600 m below the entrances, and is also found predominantly near water and in the water (B. Shade, pers. comm.).

Etymology:

The specific epithet is a noun in apposition, referring to the type locality.

Acknowledgements

Collections were made under Scientific Permit FAUT-0175 from the Secretaría de Medio Ambiente y Recursos Naturales (SEMARNAT) to O. F. Francke. We thank the participants of the Mexpe 2009 expedition to Cueva

Las Tres Quimeras, particularly Michel Cadieux, Jean-François Levis, Guillaume Pelletier, and Beverly Shade, for collecting arachnids while exploring the cave; Charles Griswold and Darrell Ubick (CAS), Gonzalo Giribet and Laura Leibensperger (MCZ), Christine Rollard and Mark Judson (MHN), the personnel (directors, researchers and assistants) of the Instituto de Investigación de Recursos Biológicos Alexander von Humboldt, Colombia (IAVH), and W. David Sissom (WDS) for lending materials and/or providing access to collections; Steve Thurston (AMNH) for assistance with preparing the plates; and Camilo Mattoni, Peter Sprouse, Bill Steele and an anonymous reviewer for comments on earlier drafts of the manuscript. Development of the original data matrix by L. Prendini was funded by grant DEB 0413453 from the National Science Foundation, USA.

References

- Armas, L. (1994). Los alacranes troglobios de México (Arachnida: Scorpionida). *Mundos subterráneos* (UMAE, México, D. F.) **5**, 18–22.
- Association for Mexican Cave Studies (AMCS) (2009a). Te Cimata, Cerro Mirador, Valle Nacional, Oaxaca. *AMCS Activities Newsletter* **32**, 61. Available online at <http://www.amcs-pubs.org/maps/1641.pdf> [Accessed on January 2014]
- Association for Mexican Cave Studies (AMCS) (2009b). ‘Oaxaca, caves’. Available online at <http://www.amcs-pubs.org/maps/Oax.html> [Accessed on January 2014]
- Beutelspacher, C.R. (2000). ‘Catálogo de los Alacranes de México’.(Morelia: Universidad Michoacana de San Nicolás de Hidalgo.)
- Bremer, K. (1994). Branch support and tree stability. *Cladistics* **10**, 295–304. doi:[10.1111/j.1096-0031.1994.tb00179.x](https://doi.org/10.1111/j.1096-0031.1994.tb00179.x)
- Comisión Nacional para el Conocimiento y Uso de la Biodiversidad (CONABIO) (2011). Geoinformación, metadatos y mapoteca digital. Available online at: <http://www.conabio.gob.mx/informacion/gis/> [Accessed on July 2009]
- Farris, J. S., Albert, V. A., Källersjö, M., Lipscomb, D., and Kluge, A. G. (1996). Parsimony jackknife outperforms neighbor-joining. *Cladistics* **12**, 99–124. doi:[10.1111/j.1096-0031.1996.tb00196.x](https://doi.org/10.1111/j.1096-0031.1996.tb00196.x)
- Fet, V., and Sissom, W. D. (2000). Family Troglotayosicidae Lourenco, 1998. In ‘Catalog of the Scorpions of the World (1758–1998)’. (V. Fet, W. D. Sissom, G. Lowe and M. E. Braunwalder.) pp. 501–502. (New York Entomological Society: New York.)
- Fitch, W. M. (1971). Toward defining the course of evolution: minimum change for a specific tree topology. *Systematic Zoology* **20**, 406–416. doi:[10.2307/2412116](https://doi.org/10.2307/2412116)
- Francke, O. F. (1977). Scorpions of the genus *Diplocentrus* from Oaxaca, Mexico (Scorpionida, Diplocentridae). *The Journal of Arachnology* **4**, 145–200.
- Francke, O. F. (1982). Studies of the scorpion subfamilies Superstitioninae and Typhlochactinae, with description of a new genus (Scorpiones, Chactidae). *Bulletin of the Association for Mexican Cave Studies* **8** / *Bulletin of the Texas Memorial Museum* **28**, 51–61.
- Francke, O. F. (1986). A new genus and a new species of troglobite scorpion from Mexico (Chactoidea, Superstitioninae, Typhlochactini). *Texas Memorial Museum. Speleological Monographs* **1**, 5–9.
- Francke, O. F. (2009). A new species of *Alacran* (Scorpiones: Typhlochactidae) from a cave in Oaxaca, Mexico. *Zootaxa* **2222**, 46–56.
- Goloboff, P. A., Farris, J. S., Källersjö, M., Oxelman, B., Ramírez, M. J., and Szumik, C. A. (2003a). Improvements to resampling measures of group support. *Cladistics* **19**, 324–332. doi:[10.1111/j.1096-0031.2003.tb00376.x](https://doi.org/10.1111/j.1096-0031.2003.tb00376.x)
- Goloboff, P. A., Farris, J. S., and Nixon, K. C. (2003b). ‘TNT: Tree Analysis Using New Technology. Computer software and documentation’. Available online at <http://www.zmuc.dk/public/Phylogeny/TNT/> [Accessed on January 2014]

- Goloboff, P. A., Farris, J. S., and Nixon, K. C. (2008). TNT, a free program for phylogenetic analysis. *Cladistics* **24**, 774–786. doi:[10.1111/j.1096-0031.2008.00217.x](https://doi.org/10.1111/j.1096-0031.2008.00217.x)
- González-Santillán, E., and Prendini, L. (2013). Redefinition and generic revision of the North American vaejovid scorpion subfamily Syntropinae Kraepelin, 1905, with descriptions of six new genera. *Bulletin of the American Museum of Natural History* **382**, 1–71.
- Graham, M., and Fet, V. (2006). Serrula in retrospect: a historical look at scorpion literature (Scorpiones: Orthosterni). *Euscorpius* **48**, 1–19.
- Hadley, A. (2008). ‘CombineZM’. Available online at <http://hadleyweb.pwp.blueyonder.co.uk/> [Accessed on January 2013]
- Hjelle, J. T. (1990). Anatomy and morphology. In ‘The Biology of Scorpions’. (Ed. G. A. Polis.) pp. 9–63. (Stanford University Press: Stanford, CA.)
- Jacob, A., Gantenbein, B., Braunwalder, M. E., Nentwig, W., and Kropf, C. (2004). Complex male genitalia (hemispermatophores) are not diagnostic for cryptic species in the genus *Euscorpius* (Scorpiones: Euscorpiidae). *Organisms, Diversity & Evolution* **4**, 59–72. doi:[10.1016/jоде.2003.11.002](https://doi.org/10.1016/jоде.2003.11.002)
- Jarvis, A., Reuter, H. I., Nelson, A., and Guevara, E. (2008). ‘Hole-filled seamless SRTM data Ver. 4, International Centre for Tropical Agriculture’. Available online at <http://srtm.csi.cgiar.org> [Accessed on September 2012]
- Kamenz, C., and Prendini, L. (2008). An atlas of book lung ultrastructure in the order Scorpiones (Arachnida). *Bulletin of the American Museum of Natural History* **316**, 1–259. doi:[10.1206/316.1](https://doi.org/10.1206/316.1)
- Klimchouk, A. (2012). Speleogenesis, hypogenic. In ‘Encyclopedia of Caves, 2nd edn’. (Eds W. B. White and D. C. Culver.) pp. 748–765. (Academic Press, Elsevier: Amsterdam.)
- Kovařík, K. (1998). Stříř (Scorpions). (Madagaskar: Jihlava). [in Czech].
- Locket, A. N. (1995). A new ischnurid scorpion from the Northern Territory, Australia. *Records of the Western Australian Museum* **52**, 191–198.
- Lourenço, W. R. (1981). Scorpions cavernicoles de l’Equateur: *Tityus demangei* n. sp. et *Ananteris ashmolei* n. sp. (Buthidae); *Troglotayosicus vachoni* n. sp. (Chactidae), scorpion troglobie. *Bulletin du Muséum National d’Histoire et Nature* **3**, 635–662.
- Lourenço, W. R. (1994). Scorpions. In ‘Encyclopedia Biospeologica 1’. (Eds C. Juberthie and V. Decu.) pp. 181–184. (Société de Biospéologie, Académie Romaine: Budapest.)
- Lourenço, W. R. (2006). Further considerations on the genus *Troglotayosicus* Lourenço, 1981 (Scorpiones: Troglotayosicidae or *Incertae sedis*). *Boletín de la Sociedad Entomológica Aragonesa* **39**, 389–395.
- Lourenço, W. R., and Francke, O. F. (1985). Révision des connaissances sur les scorpions cavernicoles (troglobies) (Arachnida, Scorpions). *Mémoires Biospéologiques* **12**, 3–7.
- Lourenço, W. R., and Sissom, W. D. (2000). Scorpiones. In ‘Biodiversidad, taxonomía y biogeografía de artrópodos de México: hacia una síntesis de su conocimiento. Vol 2’. (Eds J. Llorente Bousquets, E. González Soriano and N. Papavero.) pp. 115–135. (Universidad Nacional Autónoma de México: Mexico City.)
- Nenlin, A. B., and Fet, V. (1992). Zoogeographical analysis of the world scorpion fauna (Arachnida: Scorpiones). *Arthropoda Selecta* **1**, 3–31. [In Russian; extended English summary]
- Nixon, K. C. (2002). ‘WinClada, Version 1.00.08. Computer software and documentation’. Available online at <http://www.cladistics.com> [Accessed on July 2009]
- Prendini, L. (2000). Phylogeny and classification of the superfamily Scorpinoidea Latreille 1802 (Chelicerata, Scorpiones): an exemplar approach. *Cladistics* **16**, 1–78. doi:[10.1111/j.1096-0031.2000.tb00348.x](https://doi.org/10.1111/j.1096-0031.2000.tb00348.x)
- Prendini, L., and Wheeler, W. C. (2005). Scorpion higher phylogeny and classification, taxonomic anarchy, and standards for peer review in online publishing. *Cladistics* **21**, 446–494. doi:[10.1111/j.1096-0031.2005.00073.x](https://doi.org/10.1111/j.1096-0031.2005.00073.x)
- Prendini, L., Francke, O. F., and Vignoli, V. (2010). Troglomorphism, trichobothriaxy and typhlochactid phylogeny (Scorpiones, Chactoidea): more evidence that troglobitism is not an evolutionary dead-end. *Cladistics* **26**, 117–142. doi:[10.1111/j.1096-0031.2009.00277.x](https://doi.org/10.1111/j.1096-0031.2009.00277.x)
- Sissom, W. D. (1990). Systematics, biogeography and paleontology. In ‘The Biology of Scorpions’. (Ed. G. A. Polis.) pp. 64–160. (Stanford University Press: Stanford, CA.)
- Sissom, W. D. (2000). Family Superstitioniidae Stahnke, 1940. In ‘Catalog of the Scorpions of the World (1758–1998)’. (V. Fet, W. D. Sissom, G. Lowe and M. E. Braunwalder.) pp. 496–500. (New York Entomological Society: New York.)
- Sissom, W. D., and Cokendolpher, J. (1998). A new troglobitic scorpion of the genus *Typhlochactas* (Superstitioniidae) from Veracruz, Mexico. *The Journal of Arachnology* **26**, 285–290.
- Sissom, W. D., and Reddell, J. (2009). Cave scorpions of Mexico and the United States. *Texas Memorial Museum Speleological Monographs* **7**, 19–32.
- Smith, J. H., Jr. (2002). Hydrogeology of the Sistema Huautla karst groundwater basin. *Bulletin of the Association for Mexican Cave Studies* **9**, 1–156.
- Soleglad, M. E., and Fet, V. (2003a). The scorpion sternum: structure and phylogeny (Scorpiones: Orthosterni). *Euscorpius* **5**, 1–34.
- Soleglad, M. E., and Fet, V. (2003b). High-level systematics and phylogeny of the extant scorpions (Scorpiones: Orthosterni). *Euscorpius* **11**, 1–175.
- Stahnke, H. L. (1970). Scorpion nomenclature and mensuration. *Entomological News* **81**, 297–316.
- Steel, C. W., and White, W. B. (2012). Sistema Huautla, Mexico. In ‘Encyclopedia of Caves 2nd edn’. (Eds W. B. White and D. C. Culver.) pp. 712–718. (Academic Press, Elsevier: Amsterdam.)
- Vignoli, V., and Prendini, L. (2009). Systematic revision of the troglomorphic North American scorpion family Typhlochactidae (Scorpiones: Chactoidea). *Bulletin of the American Museum of Natural History* **326**, 1–94. doi:[10.1206/570.1](https://doi.org/10.1206/570.1)
- Volschenk, E., and Prendini, L. (2008). *Aops oncodactylus* gen. et sp. nov., the first troglobitic urodacid (Urodacidae: Scorpiones), with a reassessment of cavernicolous, troglobitic and troglomorphic scorpions. *Invertebrate Systematics* **22**, 235–257. doi:[10.1071/IS06054](https://doi.org/10.1071/IS06054)
- Volschenk, E., Locket, A. N., and Harvey, M. S. (2001). First record of a troglobitic ischnurid scorpion from Australasia (Scorpiones: Ischnuridae). In ‘Scorpions 2001. In Memoriam Gary A. Polis’. (Eds V. Fet and P. A. Selden.) pp. 161–170. (British Arachnological Society: Burnham Beeches, UK.)
- White, W. B. (2012). Hydrogeology of karst aquifers. In ‘Encyclopedia of Caves, 2nd edn’. (Eds W. B. White and D. C. Culver.) pp. 383–391. (Academic Press, Elsevier: Amsterdam.)

Appendix 1. Material examined for seven outgroup taxa for phylogenetic analysis of the typhlochactid scorpion genus, *Alacran Francke, 1982*

Specimens deposited in the following collections: American Museum of Natural History, New York (AMNH), including the Ambrose Monell Cryocollection for Molecular and Microbial Research (AMCC); California Academy of Sciences, San Francisco (CAS); Colección Nacional de Arácnidos, Instituto de Biología, Universidad Nacional Autónoma de México, Mexico City (CNAN); Instituto de Investigación de Recursos Biológicos Alexander Von Humboldt, Villa de Leyva, Colombia (IAVH); Museum of Comparative Zoology, Harvard University, Cambridge, MA (MCZ); Muséum National d'Histoire Naturelle, Paris (MNHN); W. David Sissom Private Collection, Canyon, TX (WDS)

Supersitionia donensis Stahnke, 1940: Mexico: Baja California: Municipio de Ensenada: Laguna Manuela, 34 miles NNW on road to Miller's Landing [28°12'N 114°08'W], 500 ft, S.C. Williams and M.A. Cazier, 22.vi.1968, 1 ♂, 1 ♀ (MCZ 12359). Baja California Sur: Municipio de Mulegé: Vizcaino Desert, 48 miles NW San Ignacio [27°38'N 113°22'W], S.C. Williams and C. Mullinex, 30.xi.1973, 1 ♂, 1 ♀ (CAS). Sonora: Municipio de Hermosillo: Bay New Kino, 16 km NW on dirt road, 28°55.249'N 112°02.572'W, 116 m, E. González, 2.vii.2006, UV detection at night, 1 ♀ (AMCC [LP 7679]). U.S.A: Arizona: Pinal County: Superstition Mountains, 33°25'43"N 111°25'03"W, D. Vernier, xi.2003, 1 ♂, 2 ♀ (AMCC [LP 3420]). California: San Benito County: Griswold Hills, Griswold Creek Canyon, New Idria Road, 3.7 miles S intersection with Panoche Road, 36°33'20.8"N 120°50'27.0"W, 390 m, L. Prendini, J. Huff and W. Savary, 15.ix.2007, 5 ♂ (AMNH). San Diego County: Anza-Borrego Desert State Park: Culp Valley Camp, 33°13.421'N 116°27.267'W, 1033 m, L. Prendini and R. Mercurio, 30.VIII.2005, UV light detection, 2 ♂, 1 ♀ (AMNH). Nevada: Clark County: Christmas Mountains, 35°15'39.55"N 114°44'21.97"W, 3910 ft, R.C. West, 12.x.2007, under fallen yucca trunks, 1 ♀ (AMCC [LP 7689]). Nye County: Mercury, Nevada Test Site [37°07'N 116°03'W], B.Y.U.–A.E.C. Code CBA7©, 30.x.1961, 1 ♀ (AMNH), B.Y.U.–A.E.C. Code JAL8©, 11.x.1961, 1 ♂ (AMNH). New Mexico: Hidalgo County: Granite Gap, Peloncillo Mountains, 32°05'43.1"N 108°58'13.7"W, 1367 m, L. Prendini and J. Huff, 4.ix.2007, 2 ♂, 1 ♀ (AMNH).

Troglotayosicus humiculum Botero-Trujillo and Francke, 2009: Colombia: Nariño Department: Reserva Natural La Planada, permanent plot, 01°15'N 78°15'W, 1885 m, G. Oliva, 2–4.v.2001, Winkler trap, subad. ♂ holotype (IAVH-E 100809). Ricaurte: Vereda Alto Cartagena, Finca Nueva Estrella, 01°13.262'N 77°58.143'W, R. Botero, J.P. Botero and J.A. Ochoa, 12.ix.2008, 1617 m, litter, rainforest, 1 subad. ♀, 3 juv. (AMCC [LP 9311–9314]).

Sotanochactas elliotti (Mitchell, 1971): Mexico: San Luis Potosí: Municipio de Ciudad Valles: El Sótano de Yerbaniz, 21 km N Ciudad Valles, Sierra de El Abra [22°11'07"N 98°59'12"W], ca 250 m, W.R. Elliott, 31.vii.1969, subad. ♂ holotype (AMNH), W.R. Elliott, 27.iii.1970, juv. ♀ paratype (MNHN RS 5376); R.W. Mitchell, 4.vii.1970, paratype ♂ (WDS).

Stygochactas granulosus (Sissom and Cokendolpher, 1998): Mexico: Veracruz: Municipio Tlaquilpa: Sótano de Poncho [18°37'N 97°07'W, 73 m] P. Sprouse, 22.iii.1995, juv. ♂ holotype, 1 ad., pedipalp chela only (AMNH).

Typhlochactas rhodesi Mitchell, 1968: Mexico: Tamaulipas: Municipio de Gómez Farias: La Cueva de la Mina, Sierra de Guatemala [23°06'06"N 99°12'56"W], 1600 m, 24.iii.1967, R.W. and R. Mitchell, K. Pittard, D. Falls and V. Colvin, holotype ♀ (AMNH), R.W. Mitchell, F. Abernathy and W. Rhodes, 29–30.viii.1966, subad. ♀ paratype (AMNH), R.W. Mitchell, F. Abernathy and W. Rhodes, 29.viii.1967, paratype ♀ (MNHN RS 4760).

Typhlochactas sissomi Francke, Vignoli and Prendini, 2009: Mexico: Queretaro: Municipio de Jalpan: Cañada de La Joya, 21°27'23"N 99°08'26"W, 1944 m, H. Montaño and A. Valdez, 12.vi.2004, rock-rolling, subad. ♂ holotype (CNAN T-0308), leg (AMCC [LP 2949]).

Appendix 2. Characters used for phylogenetic analysis of the typhlochactid scorpion genus, *Alacran* Francke, 1982, and seven outgroup taxa: three new and 179 from Prendini *et al.* (2009) (PEA09)

Thirty characters, indicated by †, were deactivated in the analysis. Character states are scored 0–3, ? (unknown) or - (inapplicable). Refer to Table 2 for character matrix

Pigmentation

0. †Carapace, tergites, pedipalps and metasoma (e.g. pedipalpal and metasomal carinae): infuscate (0); immaculate (1) [PEA09:1].

Chelicerae

1. Fixed finger, median and basal teeth: fused into a bicusp (conjoined on a ‘trunk’) (0); separate, not fused into a bicusp (not conjoined on a ‘trunk’) (1) [PEA09:2].
2. Movable finger, distal tooth alignment (prolateral distal and retrolateral distal teeth): opposable, prolateral distal tooth completely overlaps retrolateral distal tooth in dorsal view, U-shape in anterior aspect (0); not opposable, prolateral distal tooth does not overlap or at most partially overlaps retrolateral distal tooth in dorsal view, V-shape in anterior aspect (1) [PEA09:4].
3. Movable finger, dorsal edge, number of subdistal teeth: two (0); one (1); none (2) [PEA09:5].

Carapace

4. Anteromedian projection (epistome): absent or obsolete (0); present, well developed (1) [PEA09:6].
5. Anteromedian longitudinal sulcus: present (0); absent or obsolete (1) [PEA09:7].
6. Lateral ocelli, ‘first’ (anterior) ocellus: present, large (0); absent (1) [PEA09:8].
7. †Lateral ocelli, ‘second’ (ventromedian) ocellus: present, large (similar in size to first ocellus) (0); present, greatly reduced (much smaller than ‘first’ ocellus) (1); absent (2) [PEA09:9].
8. Lateral ocelli, ‘third’ (posterior) ocellus: present, slightly to greatly reduced (slightly to much smaller than ‘first’ and ‘second’ ocelli) (0); absent (1) [PEA09:10].
9. †Median ocelli: present (0); absent (1) [PEA09:11].

Pedipalp chela dentition

10. †Chela fingers dentition, median denticle row, primary subrows alignment: straight (0); oblique (1) [PEA09:12].
11. Chela fingers dentition, median denticle row, oblique primary subrows: not imbricated (0); imbricated (1); inapplicable (-) [PEA09:13].
12. Chela movable finger dentition, median denticle row, primary subrows: similar in length (0); basal row noticeably longer (1) [PEA09:14].
13. Chela movable finger dentition, median denticle row, first (terminal) primary subrow: absent (0); one (occasionally two) granules (1) [PEA09:15].
14. Chela movable finger dentition, number of median denticle rows: five (0); six (1); seven (2); eight (3).
15. †Chela movable finger dentition, fourth retrolateral denticle: present (0); absent (1) [PEA09:17].
16. †Chela movable finger dentition, fifth retrolateral denticle: present (0); absent (1) [PEA09:18].
17. Chela movable finger dentition, sixth retrolateral denticle: present (0); absent (1) [PEA09:19].
18. Chela movable finger dentition, seventh retrolateral denticle: present (0); absent (1) [PEA09:20].
19. Chela movable finger dentition, seventh prolateral denticle: present (0); absent (1) [PEA09:23].
20. Chela movable finger dentition, eighth prolateral denticle: present (0); absent (1) [PEA09:24].
21. Chela movable finger dentition, prolateral denticles, development relative to retrolateral denticles: prolateral denticles larger than retrolateral denticles (0); prolateral denticles smaller than retrolateral denticles (1) [PEA09:25].
22. Chela movable finger dentition, prolateral denticle development: all prolateral denticles similar in size (0); basal four prolateral denticles significantly larger (1) [PEA09:26].
23. Chela fixed finger, number of median denticle rows: five (0); six (1); seven (2).
24. Chela fixed finger, distal diastema (notch) to accommodate terminal denticle of movable finger: present, well developed (0); weakly developed or absent (1) [PEA09:27].
25. †Chela movable finger, distal diastema (notch) to accommodate terminal denticle of fixed finger: absent or weakly developed (0); present, well developed (1) [PEA09:28].
26. Chela fingers, terminus: fixed finger, terminal denticle considerably larger than preceding denticles, hook-like, fingertips interlocking unevenly when closed, movable finger markedly displaced to exterior (0); fixed finger, terminal denticle slightly larger than preceding denticles, fingertips interlocking evenly when closed, movable finger at most slightly displaced to exterior (1) [PEA09:29].

Pedipalp chela ornamentation

27. †Chela fixed finger, proximal half: smooth (0); dorsal surface granular (1); dorsal, prolateral and retrolateral surfaces granular (2) [PEA09:30].
28. †Chela fingers, curvature and closure (♂): fingers straight, fit together evenly, no gap evident when closed (0); fixed finger curved dorsally, movable finger curved ventrally, fingers fit together unevenly, distinct gap evident when closed (1); unknown (?) [PEA09:31].
29. Chela manus, prolateral surface, granulation along distal margin from base of movable finger to base of fixed finger: no prominent granules (0); row of prominent, isolated granules from base of movable finger to base of fixed finger (1); pair of prominent, isolated granules situated close together at base of fixed finger (2) [PEA09:32].
30. Chela manus, prolateral surface, granulation near movable finger condyle: no prominent granules (0); one very prominent, isolated granule (1) [PEA09:33].
31. Chela manus, dorsal secondary carina: distinct (strongly sclerotised, protruding above intercarinal surfaces) (0); obsolete (weakly sclerotised, if at all, not protruding above intercarinal surfaces) (1); absent (2) [PEA09:34].
32. Chela manus, digital carina: distinct (0); absent (1) [PEA09:35].
33. Chela manus, retrolateral secondary carina: distinct (0); obsolete (1); absent (2) [PEA09:36].
34. Chela manus, ventral retrolateral carina: distinct (0); obsolete (1); absent (2) [PEA09:37].
35. Chela manus, ventral median carina: absent (0); obsolete (1); distinct (2) [PEA09:38].
36. Chela manus, ventral median carina, one to three proximal granules in profile: present (0); absent (1) [PEA09:39].

(continued next page)

Appendix 2. (continued)

37. Chela manus, ventral prolateral carina: distinct (0); absent (1) [PEA09:40].
 38. Chela manus, ventral median and ventral prolateral carinae, relative development: ventral median carina stronger than ventral prolateral carina (0); ventral median and ventral prolateral carinae similarly developed (1) [PEA09:41].

Pedipalp patella ornamentation

39. †Patella prolateral surface, dorsal process ('dorsal patellar spur'): well developed projection comprising one or more prominent, spiniform granules (0); projection absent or very weakly developed, comprising at most a low granule (1) [PEA09:42].
 40. Patella, (dorsal) prolateral median carina ('dorsal patellar spur carina'): absent, at most one or two granules besides dorsal process ('dorsal patellar spur') (0); present, row of multiple granules (1); fully developed, granular row (2) [PEA09:43].
 41. Patella (dorsal) retrolateral median carina: obsolete (weakly sclerotised, if at all, not protruding above intercarinal surfaces) (0); absent (1) [PEA09:44].
 42. Patella (ventral) retrolateral median carina: obsolete (0); absent (1) [PEA09:45].
 43. Patella, dorsal retrolateral carina: distinct (strongly sclerotised, protruding above intercarinal surfaces) (0); obsolete (1); absent (2) [PEA09:46].
 44. †Patella, dorsal prolateral carina: obsolete (0); absent (1) [PEA09:47].
 45. Patella, ventral prolateral carina: distinct (0); obsolete (1); absent (2) [PEA09:48].
 46. Patella, ventral retrolateral carina: distinct (0); obsolete (1); absent (2) [PEA09:49].

Pedipalp femur ornamentation

47. Femur, dorsal retrolateral carina: distinct (strongly sclerotised, protruding above intercarinal surfaces) (0); obsolete (weakly sclerotised, if at all, not protruding above intercarinal surfaces) (1); absent (2) [PEA09:50].
 48. Femur, dorsal prolateral carina: distinct (0); obsolete (1); absent (2) [PEA09:51].
 49. Femur, ventral prolateral carina: distinct (0); obsolete (1); absent (2) [PEA09:52].
 50. Femur, ventral retrolateral carina: distinct, uninterrupted row of granules (0); absent (1) [PEA09:53].

Pedipalp trichobothria

51. Femur, trichobothrium i_1 : absent (0); present, full size (1) [PEA09:54].
 52. Femur, trichobothrium i_2 : absent (0); present, full size (1) [PEA09:55].
 53. †Femur, trichobothrium d_1 : absent (0); present, full size (1) [PEA09:56].
 54. Femur, trichobothrium d_2 : absent (0); present, full size (1) [PEA09:57].
 55. Femur, trichobothrium d_3 : absent (0); present, full size (1) [PEA09:58].
 56. Femur, trichobothrium d_4 : absent (0); present, full size (1) [PEA09:59].
 57. Femur, trichobothrium d_5 : absent (0); present, full size (1) [PEA09:60].
 58. Patella, trichobothrium d_1 : present, petite (0); present, full size (1) [PEA09:61].
 59. Patella, trichobothrium d_2 : present, petite (0); present, full size (1) [PEA09:62].
 60. Patella, trichobothrium i_1 : absent (0); present, full size (1) [PEA09:63].
 61. Patella, trichobothrium i_2 : absent (0); present, full size (1) [PEA09:64].
 62. Patella, trichobothrium v_2 : absent (0); present, full size (1) [PEA09:65].
 63. †Patella, trichobothrium v_3 : absent (0); present, full size (1) [PEA09:66].
 64. Patella, trichobothrium v_4 : absent (0); present, full size (1) [PEA09:67].
 65. †Patella, trichobothrium v_5 : absent (0); present, full size (1).
 66. Patella, trichobothrium et_1 : absent (0); present, full size (1) [PEA09:68].
 67. Patella, trichobothrium et_2 : absent (0); present, petite (1); present, full size (2) [PEA09:69].
 68. Patella, trichobothrium et_3 : absent (0); present, petite (1); present, full size (2) [PEA09:70].
 69. Patella, trichobothrium et_4 : absent (0); present, full size (1) [PEA09:71].
 70. Patella, trichobothrium et_5 : absent (0); present, petite (1); present, full size (2) [PEA09:72].
 71. Patella, trichobothrium et_6 : absent (0); present, full size (1). [PEA09:73]
 72. Patella, trichobothrium et_7 : absent (0); present, full size (1). [PEA09:74]
 73. Patella, trichobothrium et_8 : absent (0); present, full size (1). [PEA09:75]
 74. Patella, trichobothrium et_9 : absent (0); present, full size (1); polymorphic 0,1 [PEA09:76].
 75. Patella, trichobothrium est_2 : absent (0); present, full size (1) [PEA09:77].
 76. Patella, trichobothrium em_2 : absent (0); present, full size (1) [PEA09:78].
 77. Patella, trichobothrium em_3 : absent (0); present, full size (1) [PEA09:79].
 78. Patella, trichobothrium em_4 : absent (0); present, full size (1) [PEA09:80].
 79. Patella, trichobothrium esb_2 : absent (0); present, petite (1); present, full size (2) [PEA09:81].
 80. Patella, trichobothrium esb_3 : absent (0); present, petite (1); present, full size (2) [PEA09:82].
 81. Patella, trichobothrium esb_4 : absent (0); present, petite (1); present, full size (2) [PEA09:83].
 82. Patella, trichobothrium esb_5 : absent (0); present, full size (1) [PEA09:84].
 83. Patella, trichobothrium eb_1 : absent (0); present, full size (1) [PEA09:85].
 84. †Patella, trichobothrium eb_2 : absent (0); present, petite (1); present, full size (2) [PEA09:86].
 85. Patella, trichobothrium eb_3 : absent (0); present, petite (1); present, full size (2) [PEA09:87].
 86. Patella, trichobothrium eb_4 : absent (0); present, full size (1) [PEA09:88].
 87. Patella, trichobothrium eb_5 : absent (0); present, full size (1) [PEA09:89].
 88. Patella, trichobothrium eb_6 : absent (0); present, full size (1) [PEA09:90].
 89. Patella, trichobothrium eb_7 : absent (0); present, full size (1) [PEA09:91].

(continued next page)

Appendix 2. (continued)

-
90. Patella, trichobothrium eb_8 : absent (0); present, full size (1) [PEA09:92].
 91. Patella, trichobothrium eb_9 : absent (0); present, full size (1) [PEA09:93].
 92. Chela, trichobothrium i_1 : absent (0); present, full size (1) [PEA09:94].
 93. Chela, trichobothrium i_2 : absent (0); present, full size (1) [PEA09:95].
 94. †Chela, trichobothrium i_3 : absent (0); present, full size (1) [PEA09:96].
 95. Chela, trichobothrium i_4 : absent (0); present, full size (1) [PEA09:97].
 96. Chela, trichobothrium V_1 : present, petite (0); present, full size (1) [PEA09:98].
 97. Chela, trichobothrium V_2 : absent (0); present, full size (1) [PEA09:99].
 98. Chela, trichobothrium V_3 : absent (0); present, full size (1) [PEA09:100].
 99. Chela, trichobothrium V_4 : absent (0); present, full size (1) [PEA09:101].
 100. Chela, trichobothrium V_5 : absent (0); present, full size (1) [PEA09:102].
 101. Chela, trichobothrium V_6 : absent (0); present, full size (1) [PEA09:103].
 102. Chela, trichobothrium Esb_1 : present, petite (0); present, full size (1) [PEA09:104].
 103. Chela, trichobothrium Esb_2 : absent (0); present, full size (1) [PEA09:105].
 104. Chela, trichobothrium D_1 : present, petite (0); present, full size (1) [PEA09:106].
 105. †Chela, trichobothrium D_2 : absent (0); present, full size (1) [PEA09:107].
 106. †Chela, trichobothrium D_3 : absent (0); present, full size (1) [PEA09:108].
 107. †Chela, trichobothrium Et_3 : absent (0); present, petite (1) [PEA09:109].
 108. Chela, trichobothrium Et_4 : absent (0); present, petite (1); present, full size (2) [PEA09:110].
 109. Chela, trichobothrium Et_5 : absent (0); present, full size (1) [PEA09:111].
 110. Chela, trichobothrium Et_6 : absent (0); present, full size (1) [PEA09:112].
 111. †Chela, trichobothrium Est_4 : absent (0); present, full size (1) [PEA09:115].
 112. †Chela, trichobothrium Est_5 : absent (0); present, full size (1) [PEA09:116].
 113. Chela, trichobothrium Est_6 : absent (0); present, petite (1); present, full size (2) [PEA09:117].
 114. †Chela, trichobothrium Est_7 : absent (0); present, full size (1) [PEA09:118].
 115. Chela, trichobothrium d_2 : absent (0); present, full size (1) [PEA09:119].
 116. Chela, trichobothrium d_3 : absent (0); present, full size (1) [PEA09:120].
 117. Chela, trichobothrium d_4 : absent (0); present, full size (1) [PEA09:121].
 118. Chela, trichobothrium d_5 : absent (0); present, full size (1) [PEA09:122].
 119. †Chela, trichobothrium d_6 : absent (0); present, full size (1) [PEA09:123].
 120. Chela, trichobothrium d_7 : absent (0); present, petite (1); present, full size (2) [PEA09:124].
 121. Chela, trichobothrium d_8 : absent (0); present, petite (1); present, full size (2) [PEA09:125].
 122. Chela, trichobothrium m_1 : absent (0); present, full size (1) [PEA09:126].
 123. Chela, trichobothrium m_2 : absent (0); present, full size (1) [PEA09:127].
 124. Chela, trichobothrium m_3 : absent (0); present, full size (1) [PEA09:128].
 125. Chela, trichobothrium m_4 : absent (0); present, petite (1); present, full size (2) [PEA09:129].
 126. Chela, trichobothrium e_2 : absent (0); present, full size (1) [PEA09:130].
 127. Chela, trichobothrium e_4 : absent (0); present, full size (1) [PEA09:131].
 128. †Chela, trichobothrium e_5 : present, petite; present, full size (1) [PEA09:132].
 129. Chela, trichobothrium e_6 : absent (0); present, petite (1); present, full size (2) [PEA09:133].
 130. Chela, trichobothrium e_7 : absent (0); present, full size (1) [PEA09:134].
 131. Chela, trichobothrium e_8 : absent (0); present, full size (1) [PEA09:135].
 132. Patella, trichobothrium v_1 , position relative to trichobothrium esb_1 : proximal to (0); level with (1); distal to (2) [PEA09:136].
 133. Chela, trichobothrium d_4 , position relative to trichobothrium e_5 : distal to (0); level with (1); inapplicable (-) [PEA09:137].

Legs

134. Legs I–IV, prolateral pedal spurs: present (0); absent (1) [PEA09:138].
 135. Legs I–IV, retrolateral pedal spurs: present (0); absent (1) [PEA09:139].
 136. Basitarsi I–III, retrolateral spinules or spinule clusters: absent (0); short distal row (1); long, well developed continuous row (2) [PEA09:141].
 137. Basitarsus (IV), retrolateral spinules or spinule clusters: absent (0); distal spinules or spinule clusters only (1) [PEA09:142].
 138. Basitarsi I and II, proventral spinules or spinule clusters: absent (0); short subdistal row (1); long row, at least half length of segment (2) [PEA09:146].
 139. Telotarsi, ventral surface, spinules or spinule clusters, curved proximal row: present (0); absent (1) [PEA09:149].
 140. Telotarsi, ventral surface, spinules or spinule clusters, straight ventromedian row: present (0); absent (1) [PEA09:150].
 141. Telotarsi, ventral surface, spinules or spinule clusters, number of ventrodistal pairs: more than three (0); none (1) [PEA09:151].
 142. Telotarsi, ventral surface, spinules or spinule clusters, rows flanking pseudonychium (dactyl): absent (0); present (1) [PEA09:152].
 143. Telotarsi, ventral surface, spinules, type: simple, isolated spinules (0); loose clusters of elongated spinules (1); inapplicable (-) [PEA09:153].
 144. Telotarsi, ventral macrosetae, arrangement: irregularly arranged, ‘non-flanking’ (0); regularly arranged into pair of distinct ventrosubmedian rows (1) [PEA09:154].
 145. Telotarsi, ventral macrosetae, development: thin, acuminate (0); subspiniform (1) [PEA09:155].
 146. Telotarsi, ventrosubmedian (‘flanking’) setal pairs, number: 3–5 (0); 6–8 (1); more than 10 (2) [PEA09:156].

(continued next page)

Appendix 2. (continued)**Sternum**

147. Sternum, vertical compression: absent, length greater than or equal to posterior width (0); minimal, length less than width (1) [PEA09:157].
 148. Sternum apex, shape: pointed (0); rounded (1) [PEA09:158].
 149. Sternum lateral lobes, development: strongly convex (lobes create deep cleft medially) (0); weakly convex (lobes create shallow cleft medially) (1); flat (2) [PEA09:159].

Tergites

150. †Tergite VII, dorsal submedian carinae, longitudinal development: vestigial (few posterior granules) (0); absent (1) [PEA09:160].
 151. Tergite VII, dorsal lateral carinae, longitudinal development: distinct, complete (0); vestigial (few posterior granules) (1); absent (2) [PEA09:161].

Pectines

152. †Pectinal fulcra, development: well developed (0); absent (1) [PEA09:163].
 153. Pectinal lamellae, sutures, transverse suture between second (subdistal) and third marginal lamellae: present, lamellae separated (0); absent, lamellae fused (1) [PEA09:164].
 154. Pectinal lamellae, sutures, longitudinal suture between second (subdistal) marginal lamella and second (subdistal) or second and third medial lamellae: present, lamellae separated (0); absent, lamellae fused (1) [PEA09:165].
 155. †Pectinal lamellae, sutures, transverse suture between second (subdistal) and third medial lamellae: present, lamellae separated (0); absent, lamellae fused (1) [PEA09:166].
 156. Pectinal lamellae, sutures, transverse suture between third and fourth medial lamellae: present, lamellae separated (0); absent, lamellae fused (1) [PEA09:167].
 157. Pectinal lamellae, sutures, transverse suture between fourth and fifth medial lamellae: present, lamellae separated (0); absent, lamellae fused (1) [PEA09:168].
 158. Pectines, proximal medial lamella (scape), angle (♂): acute, less than 90° (0); approximately 90° (1); obtuse, greater than 90° but less than 180° (2); unknown (?) [PEA09:169].
 159. †Pectinal teeth, number (♂): 5 (0); 6 (1); 7 (2); unknown (?) [PEA09:172].
 160. Pectinal teeth, number (♀): 5 (0); 6 (1); 7 (2); polymorphic (0 1); unknown (?) [PEA09:173].
 161. Pectinal teeth, shape: curved, slightly overlapping (0); straight, non-overlapping (1) [PEA09:174].

Sternites

162. Sternite VII, ventral lateral carinae: present (0); absent (1) [PEA09:176].
 163. †Stigmata, shape: oval (0); round (1) [PEA09:177].

Metasoma

164. Metasomal segments I–III, dorsal submedian carinae: distinct (strongly sclerotised, protruding above intercarinal surfaces) (0); obsolete (weakly sclerotised, if at all, not protruding above intercarinal surfaces) (1) [PEA09:178].
 165. Metasomal segments I–III, dorsal submedian carinae, posterior granules: not noticeably larger than preceding granules (0); significantly larger than preceding granules (1) [PEA09:179].
 166. Metasomal segment IV, dorsal submedian carinae: distinct (0); obsolete (1) [PEA09:180].
 167. Metasomal segments I–III, dorsal lateral carinae: distinct (0); obsolete (1); absent (2) [PEA09:181].
 168. Metasomal segment IV, dorsal lateral carinae: distinct (0); absent (1) [PEA09:182].
 169. Metasomal segment V, dorsal lateral carinae: distinct (0); obsolete (1) [PEA09:183].
 170. Metasomal segments I, dorsal lateral carinae, longitudinal development: present, complete (extending full length of segment) (0); present, incomplete (not extending full length of segment) (1); absent (2) [PEA09:184].
 171. Metasomal segments II and III, dorsal lateral carinae, longitudinal development: present, complete (0); present, incomplete (1); absent (2) [PEA09:185].
 172. Metasomal segment I, median lateral carinae, longitudinal development: present, incomplete (0); absent (1) [PEA09:186].
 173. Metasomal segment II, median lateral carinae, longitudinal development: present, incomplete (0); absent (1) [PEA09:187].
 174. Metasomal segment III and IV, median lateral carinae, longitudinal development: present, incomplete (0); absent (1) [PEA09:188].
 175. Metasomal segment I, ventral lateral carinae: distinct (0); obsolete (1); absent (2) [PEA09:189].
 176. Metasomal segments II–IV, ventral lateral carinae: distinct (0); obsolete (1); absent (2) [PEA09:190].
 177. Metasomal segment V, ventral lateral carinae: distinct (0); obsolete (1); absent (2) [PEA09:191].
 178. Metasomal segment V, ventral lateral carinae, longitudinal development: complete (0); restricted to distal third of segment (1); inapplicable (-) [PEA09:192].
 179. †Metasomal segment V, ventral median carina: obsolete (0); absent (1) [PEA09:193].

Telson

180. Telson vesicle, width relative to metasomal segment V, distal width: broader than (0); similar to (1) [PEA09:194].
 181. Telson vesicle, anterodorsal lateral lobes: present (0); absent (1) [PEA09:195].